IEEE Access
Multidisciplinary ⋮ Rapid Review ⋮ Open Access Journal

Received 25 July 2023, accepted 8 August 2023, date of publication 15 August 2023, date of current version 24 August 2023.

Digital Object Identifier 10.1109/ACCESS.2023.3305674

TOPICAL REVIEW

Review of the Evolution of Magnetorheological Fluid-Based Rehabilitative Devices: From the Perspective of Modeling, Sensors and Control Strategies

AKHILA BHAT[1], VIDYA S. RAO[1], (Member, IEEE), AND N. S. JAYALAKSHMI[2], (Senior Member, IEEE)

[1]Department of Instrumentation and Control Engineering, Manipal Institute of Technology, Manipal Academy of Higher Education, Manipal, Karnataka 576104, India

[2]Department of Electrical and Electronic Engineering, Manipal Institute of Technology, Manipal Academy of Higher Education, Manipal, Karnataka 576104, India

Corresponding author: Vidya S. Rao (rao.vidya@manipal.edu)

ABSTRACT Over the past decade, rehabilitative devices have undergone significant advancements. Orthoses, which are assistive limb devices, have transitioned from passive supportive devices to active or semiactive devices with adjustable damping. Similarly, prosthetic limb-replacement devices for amputees have shifted towards the integration of semiactive dampers instead of passive or bulky dampers. The implementation of semiactive damping is achieved through the use of smart magnetorheological (MR) fluids that can modify their viscosity based on the input current, resulting in reduced power consumption. This article focuses mainly on modelling, sensors and control strategies in MR damper-based rehabilitative devices since these areas contribute to the development of the overall end product. There have been notable improvements in the modelling of human knee joints and the damping system components, aiming to achieve more efficient damping control. Traditional mathematical equations, such as Lagrangian and Newtonian formulations, have been supplemented with machine learning algorithms. Additionally, the utilization of various sensor combinations to measure knee/ankle joint angles has advanced. These sensors range from basic mechanical sensors to wireless inertial and piezoelectric sensors, enabling faster and more diverse communication. Furthermore, control algorithms have also witnessed a progression from classical control approaches to more sophisticated strategies such as fuzzy control and neural network controllers. These advanced control algorithms enhance the overall performance and responsiveness of the rehabilitative devices. However, there are certain disadvantages found in MR fluids, sensors, modelling and control algorithms that are discussed further in this review article. This review explores the developments in different rehabilitative devices that integrate modelling, sensors, and control designs to achieve optimal and efficient outcomes.

INDEX TERMS Modeling, MR damper, orthosis, prosthesis, sensors, semiactive controller.

I. INTRODUCTION

Orthosis or braces are appliances that are applied externally to assist and resist movements and can unload, accommodate and support segments of the body [1], [2]. Bracing of the lower limb joints, especially for the knee and ankle, is in practice for several reasons, such as to increase proprioception, to prevent injuries, especially in contact sports and sports involving jumping and landing, to protect the healing ligaments and soft tissues during rehabilitation from injuries and to be therapeutic, as in cases of acute injuries or in inflammatory or degenerative arthritis in the aged population. Various passive braces or orthotic supports prescribed in various conditions with several indications, as shown in Fig. 1,

The associate editor coordinating the review of this manuscript and approving it for publication was Qi Zhou.

FIGURE 1. Types of passive knee orthoses [1].

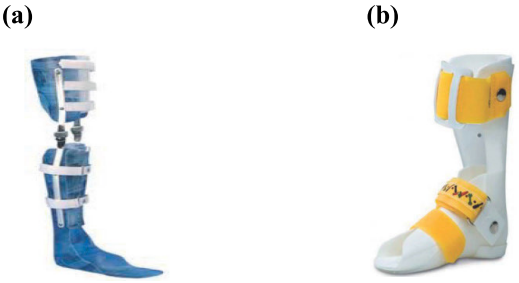

FIGURE 2. Passive orthoses (a) for knee and (b) for ankle [3].

may range from protective braces to resist movement and support the limb that is damaged due to degeneration or post traumatic conditions such as degenerative arthritis/post traumatic arthritis [3], [4], [5]. Knee sleeves are used to provide compression during minor injuries. Rehabilitative braces are used to support the limb resisting unwanted movements and assisting locomotion, such as in rehabilitation movements and assisting locomotion, such as in rehabilitation of ligamentous injury in movements and assisting locomotion, as in rehabilitation of ligamentous injury in recovery stage either following nonoperative treatment or following surgical intervention for example post anterior cruciate ligament injuries in knee joint, postsurgical intervention for instability at ankle joint. Functional braces allow full range of movement at the joint but with additional support to prevent injuries. Bracing is worn as a protective aid during a sporting activity that involves cutting and jumping movements, such as in soccer, tennis, basketball, etc. Varieties of ankle foot orthoses, knee-ankle-foot orthoses for knee and ankle joints, spinal orthoses for neck and spine, wrist-hand orthoses and powered elbow wrist-hand orthoses for wrist and elbow joints, mobility aids are discussed [3], [6], [7], [8].

This section provides an overview of the evolution in orthotic devices and prosthetic devices and application of MR fluid in these devices. The earlier orthotic and prosthetic devices were passive with limited fixed range of damping. But incorporating them with sensors, smart actuators and advanced control algorithms resulted in sophisticated customized devices. One such device is MR fluid based rehabilitative device that alters the damping output of the actuator based on the input current provided, in turn to give variable damping at the lower or upper limb joint so as to restrict its movement.

In [3], the authors discussed muscle diseases such as distal, atrophy, myositis, carnitine deficiency, and congenita that require lower and upper extremity orthoses. Upper and lower extremity orthoses are preferred for many muscular disorders in the elbow, wrist, spine, ankle, and knee for maintaining range of motion and steady balance and preventing contractures, thus delaying surgery. Post stroke, the plantar flexion and dorsiflexion movements of the ankles are severely affected in individuals, resulting in nonuniform gait [9].

To overcome this, several ankle foot orthoses have been discussed for rehabilitation and metabolic cost reduction during walking [3], as shown in Fig. 2. The rehabilitative type includes passive, active and semiactive orthoses, and the metabolic cost-reducing type includes exoskeletons. The orthoses will be a combination of sensors, actuators, power sources and control units. The weight of the orthoses varies from 0.53 kg to 4 kg. The sensors may be motion capture systems, EMG sensors, angle sensors, force sensors, and orientation sensors. Patients with paretic ankle need torque at the propulsive gait phase; hence, active and passive braces are preferred. According to [10], orthoses affect the lower limb calf muscles, such as the tibialis posterior (TP), flexor digitorum longus (FDL), and peroneus longus (PL) [11]. Fine-wire and surface electromyography (EMG) sensors and force plates were employed to measure muscle activity and gait phase, respectively. Sixteen participants were chosen for the study, and three running trials were conducted on barefoot, footwear and footwear with orthosis. The EMG signals were captured in the stance gait phase during all the trials, and measurements from only eight participants were chosen for further analysis. Although there were no significant differences in FDL and PL EMG signals, TP muscle activity was reduced while the orthosis was worn. A commercial ankle foot orthosis (AFO) for patients affected by stroke is combined with trunk orthosis that was previously developed by the same authors [12]. A motion capture system was used to obtain kinematic gait data. Twenty-eight stroke patients were chosen for the study and were divided into two groups: one group with AFO plus trunk orthosis and the other with AFO plus corset. The AFO plus trunk orthosis group performed better during the walking test in terms of walking speed, steps per minute in the affected foot and peak ankle plantar flexion angle during the stance gait phase. Previously developed powered orthoses were primarily tethered while aiding the limb, but in [13] and [14], portable electric and pneumatic orthoses were developed. In [13], the device helped in dorsi and plantar flexion using control from embedded electronics that depend on foot force sensors. However, size is an issue of concern, and future developments should focus on minimizing size and, ultimately, weight to increase patient compliance, which is reflected in Fig. 3.

In [15], the authors developed a fabricated orthosis with a motor that assists patients with paraplegia and causes synchronized movement of the hip and knee joint. The

FIGURE 3. Pneumatic portable orthosis [13].

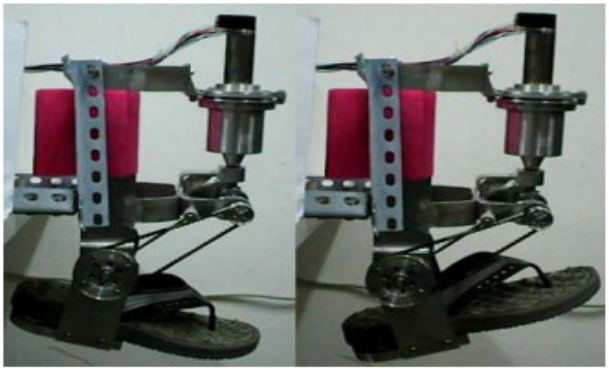

FIGURE 4. Orthosis with electric motor [16].

previously proposed orthoses were bulky and inconvenient with pneumatic and hydraulic actuators, which even provided insufficient power; thus, this device helps overcome these limitations. The orthosis could provide improvement in gait in terms of speed and balance. To further improve patient convenience as well as the weight of the orthosis, the authors of [16] developed a gear-based ankle orthotic for assistance with dorsi and plantar flexion that consists of an electric motor controlled via a proportional-integral-derivative (PID) controller, as shown in Fig. 4. The PID controller was responsible for position and speed control based on the state of the force sensors. However, there was room for improvement in the use of other gait parameters, including the use of injured foot pressure sensor data rather than healthy individuals' foot data for obtaining the control curve, additional torque production for the ankle and soft sensing systems for locking and braking.

Several devices for tremor suppression were discussed based on their functionality. Transcutaneous Electrical Nerve Stimulators, Functional Electrical Stimulators, wearable active and semiactive and orthoses, assistive feeding devices, gyroscopic stabilizers and haptic stimulation systems were assessed [6], [17], [18], and an example from [17] is shown in Fig. 5.

The study evaluated the devices based on efficiency and potential risks. Noninvasive tremor-suppressing devices were

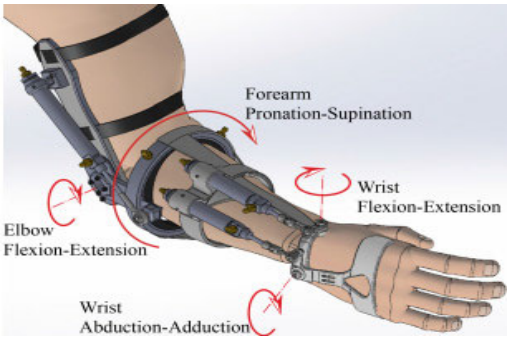

FIGURE 5. Tremor suppression upper limb orthosis [17].

preferred over invasive transcutaneous devices. Additionally, the devices could provide 30-99.8% tremor suppression. However, passive orthoses provide adequate damping only when static and certain dynamic activities are performed. When dynamic activities are involved, such as brisk walking, running, ascent or descent of stairs, additional assistance in the form of torque is required to the affected limb.

As in [7], a random crossover design was used, and two orthoses, a prefabricated orthosis and a sham foot orthosis, were compared. The ground reaction force variables (cushioning of forefoot and heel, arch support) and subjective opinions (visual analogue scale) were obtained by twenty male athletes with flat foot. The participants were made to run on an instrumented treadmill for 5 s at each speed (5, 6 and 7 m/s), gradually increasing at a rate of 0.4 m/s2 with each foot orthosis. The data recorded were processed in MATLAB, and statistical analysis (ANOVA, t test between speed and orthosis) was carried out in SPSS software. After using prefabricated foot orthosis, there was an increase in the vertical impact force, loading rate, and kinetic variability of the peak propulsive force while running from lower to higher speeds. Prefabricated foot orthosis gave better arch support but less forefoot and heel cushioning and overall comfort. As illustrated in Fig 6, an ankle foot orthosis was used in patients with drop foot conditions [8]. Nineteen patients were chosen for the study and classified into the robotic group (active powered ankle assistance) and the sham group (passive torque impedance for 10) based on a double-blinded randomized controlled trial. The inclusion criteria were assessed by functional ambulatory category ≥ 4 and Berg balance scale ≥ 40, and the exclusion criteria included range of motion evaluated by modified Ashworth scale ≥ 3. Evaluations were performed before and after the 20-session gait training (30-minute level walk and stair ascent) with follow-ups every 3 months. After the training test, the robotic group performed well in terms of gait improvement, walking speed, loading response of the affected side and prevention of flat foot ground contact.

To achieve additional active torque during ascent, a ball screw mechanism was used, which was driven by a motor and hydraulic damper-based prosthesis [19], as shown in Fig. 6. Inspired by a healthy knee, a four-bar link was designed to simulate the prosthetic knee, as shown in Fig. 7. The

FIGURE 6. Robotic orthosis for drop foot [8].

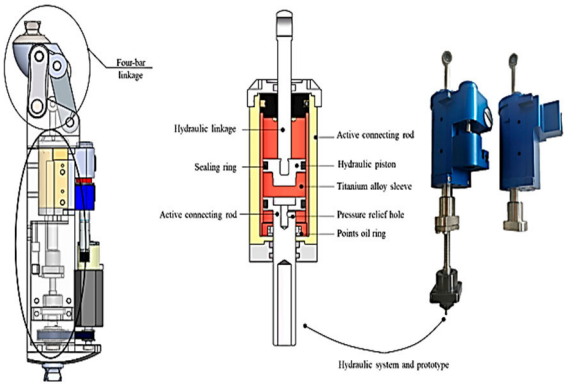

FIGURE 7. Four bar link knee prosthesis [19].

simulation was carried out in ADAMS software, and the proposed algorithm provided a 10% torque symmetry index and 34.7% and 11.5% knee angle symmetry index in the stance and swing phases, respectively. The results were comparable with the healthy knee, and the proposed knee outperformed other previous works in terms of active torque generation and overall weight. Similarly, in [20], a five-bar link prosthesis was proposed by the authors.

In [21], a crossover study design was carried out to compare four conditions, i.e., shoes only, a commercially produced carbon fibre ankle foot orthosis, a custom-made carbon fibre ankle foot orthosis and a powered orthosis with a series-elastic actuator. The mechanical efficiency and net metabolic costs were some of the evaluated parameters assessed by effect sizes (d, where $d>0.8$ signified better performance). Three subjects with lower-limb reconstruction were chosen for the study and were made to walk at different speeds in four conditions. Although the powered ankle foot orthosis outperformed other conditions in net positive work ($d\geq1.17$) and efficiency ($d\geq1.43$), patients still considered nonpowered orthosis since the weight of the orthosis was a drawback.

The paper is divided into three major sections. Section II describes the evolution of the modelling of knee joints and MR dampers. Section III discusses the advancements in the sensors used in orthotic and prosthetic devices. Section IV consists of the progress in the control algorithms applied in rehabilitative devices over the last decade.

The advancement in prosthetic knees from 2010 to 2020 has been discussed in the area of structure and control strategy in [22]. Various designs of prostheses, such as uniaxial, multiaxial, with and without locking mechanisms, and four bar links with MR dampers for swing control, have been discussed. In [23], the authors provided a detailed review of various passive, active and semiactive ankle foot orthoses, data collection for achieving good control in orthoses, and data interfacing with the wearer. Passive orthoses are preferred for simple activities since the damping is fixed, but semiactive and active orthoses are necessary for difficult walking or pacing conditions since the damping varies according to the angle of the ankle joint. Rigid actuators such as motor, hydraulic and MR dampers and elastic actuators with series and parallel configurations for less energy consumption [24], [25] are explained. The article explains the control algorithms for gait phase recognition using EMG sensors. The evolution of the prosthesis can be perceived in terms of weight reduction of the prosthesis, advanced control algorithms for damping using cost-effective elastic actuators and actuators, and easy adaptability for patients. Single segmented rehabilitation devices (for shoulder, elbow, forearm, wrist, finger/s) and multisegmented rehabilitation devices (shoulder-elbow, wrist-finger, forearm-wrist, shoulder-elbow-forearm) have been described [26]. High-level control (assistive, task, haptic interface, noncontact monitoring control) and low-level control (linear-PD, PID and nonlinear-adaptive, impedance, sliding mode controllers) have been discussed. The actuators can be classified into hydraulic, pneumatic and electric, and devices can be stationary, portable or wearable. The various assisting modes are active/passive assist, active assist and resist passive assist and resist. Prominent control inputs include EMG, position, force, joint angles and torque.

Since variable damping is preferred over passive damping (fixed braking for both static and dynamic activities) and active damping (more power consumption), smart fluids such as electrorheological (ER) and MR fluids are used in dampers. The MR damper is a component that has MR fluids consisting of micron-sized ferrous particles suspended in carrier liquids. The carrier fluid goes to a semisolid state under the influence of a magnetic field since the ferrous particles in the fluid align themselves in the direction of magnetic lines of force, in turn increasing the resistance or viscosity. The resistance decreases when the magnetic field is removed, with the fluid reversing to the liquid state, behaving like a Newtonian fluid [27], [28], [29]. This property is used to create vibration isolation in structures, braking in automobile suspensions, prostheses, cable bridges, washing machines, etc. In biomedical applications such as knee prostheses and haptic and tactile devices, the MR damper is employed to provide braking and shock absorption to mimic the functions of damping in the human leg.

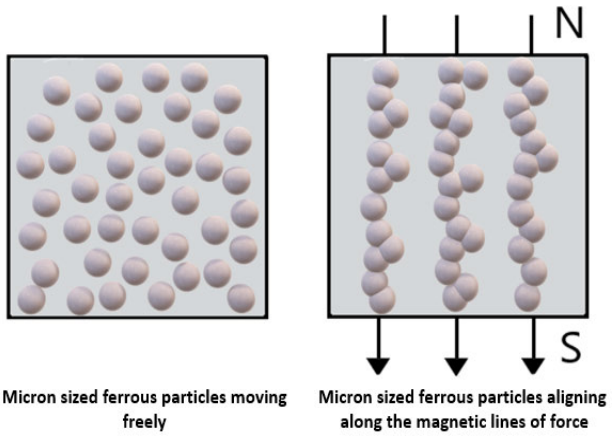

FIGURE 8. MR fluid particle behavior [27].

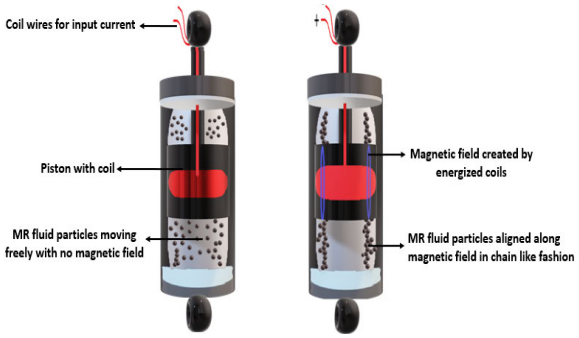

FIGURE 9. MR damper fluid behavior in the presence of magnetic field [27].

When a magnetorheological (MR) damper, which has a response time of only a few milliseconds, is incorporated in the aforementioned braces. It increases the compliance to the braces as well as the efficiency of the individual's locomotion. The yield strength of the MR damper is controlled by altering the viscosity of the damper fluid, as seen in Fig. 8, rather than having fixed damping as seen in passive dampers; thus, MR damping is considered to be semiactive damping, as shown in Fig. 9, as well as efficiency of the individual's locomotion. having fixed damping as seen in passive dampers, thus, MR damping is considered to be semiactive damping.

The characteristics of ER fluids, MR fluids and shape memory alloys are thoroughly discussed [27], [30]. The ER and MR fluids are smart fluids with suspended colloidal materials excited by electrical and magnetic fields, thus altering their viscosity. Shape memory alloys are alloys that change their shape and return to normal based on the heat applied. These features of the materials are applied in robotics, biorobots and automobile industries. Applications of ER fluids include tactile displays, flexible robotic arms, gantry robots, orthoses, and manipulators. MR fluids are used in vehicle shock absorption, robot manipulators, grippers, prostheses, haptic robots, rehabilitation, climbing robots, leg robots and building dampers [31], [32]. Although ER fluids exhibit a relatively faster response time than MR fluids, ER fluids require a high voltage power supply to generate the electric field necessary for their response. This may limit their use in certain portable or battery-powered applications. MR fluids require a lower power supply, typically in the range of a few volts, making them more suitable for portable and low-power applications, which allows for the use of simpler and more compact magnetic actuation systems in orthotic or prosthetic devices.

Shape memory alloys are applied in bioinspired robots such as microfish, jumping, buoyance, flying and swimming robots [34], [35]. In [36], the wide applications of MR fluids in engineering and medical fields are discussed. From 2018-2020, in engineering fields, MR clutches, MR brakes, MR mounts and in medical fields have been extensively used in haptic devices and rehabilitative devices in flow, squeeze or shear modes [37], [38]. By altering the properties of the MR damper coil, there will be certain advantages, such as a quicker response with replacement using a permanent magnet or by increasing turns. However, these changes will also add more weight to the structure. Additionally, the combination of modes of the MR damper can be beneficial for energy savings. In [39], the Newtonian properties of the MR fluid, operation modes and evolution of MR devices were discussed. MR fluid devices operate in flow mode, shear mode or squeeze mode, and the combination of these modes is found in recent applications such as mounts, shock absorbers and servo valves. The relationship between magnetic flux density and shear stress has been depicted using the Bingham plastic model. MR fluid applications have evolved from MR dampers, MR valves [40], [41], [42], MR mounts [43] and MR brakes from 2001 to 2015. A systematic review of MR damper fluid properties, operational modes, and dynamic models is carried out [44]. Classic, advanced and intelligent control strategies of MR damping systems in various applications are brought to attention. Since the MR damper dynamic model is nonlinear, model accuracy plays a key role, and advanced control algorithms give better performance for bionic [45], [46] and structural vibration attenuation. Electronically commutated (EC) motors with MR clutches and MR brakes are both used in the prosthesis as actuators and dampers [47], which is highlighted in Fig. 10. Similar work was carried out in an MR damper with flow mode and EC motor, with a nonlinear proportional derivative controller in [33], and these operate individually or together based on the phase of the gait cycle.

In [47] and [48], dynamic models of the MR clutch and brake were derived and tested experimentally to obtain a model from the MATLAB identification toolbox. A proportional-integral (PI) controller was also designed to control the clutch and braking, as depicted in Fig. 11. For ground level walking, the proposed device with both motor reducer plus MR brake/clutch (active), with only motor reducer unit and only MR brake (semiactive) unit was compared. The semiactive mode with only the MR brake required only 6.0 J of energy, the MR clutch/brake combination

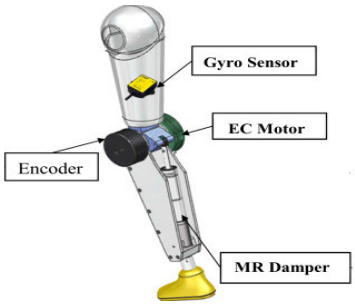

FIGURE 10. Knee prosthesis with MR damper [33].

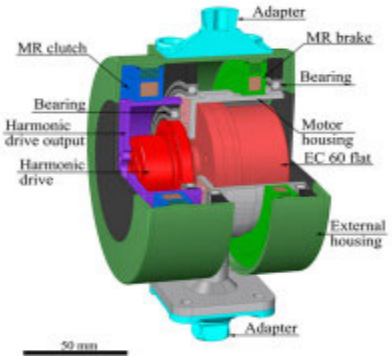

FIGURE 11. MR brake and clutch for knee prosthesis [47].

FIGURE 12. Ankle orthosis with MR fluid-based damper [51].

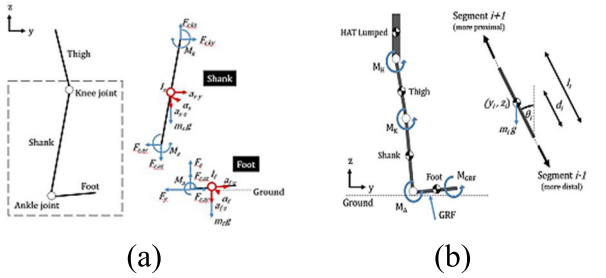

FIGURE 13. Human lower limb model (a) Newtonian (b) Lagrangian [52].

required 16.3 J, and the active mode with the motor reducer required 26.6

Angle sensors, strain gauge sensors and accelerometers were used to measure the flexion angle, ground reaction force and gait posture [49]. The microprocessor controls the hydraulic damper used for braking. In the article mentioned, the method is compared with the hydraulic-based Otto Bock C-leg, Mauch prosthetic knee and MR fluid-based Ossur Rheo in terms of energy cost, gait efficiency and exercise intensity tested on the MasterScreen testing system. Ten amputees with ages ranging from 20-45 who have been using prosthetics from 1-15 years. Analysis of variance (ANOVA) was used to analyse the significance between the tests performed at different speeds (0.5, 0,7, 0.9, 1.1 and 1.3 m/s). There was no significant difference in energy cost or gait efficiency for the four prosthetic knees. However, the Mauch SNS underperformed compared to the other three prosthetic knees. A similar retrospective study was conducted by the authors in [50] with four microprocessor-based prosthetic knees, namely, C-leg (hydraulic damping), Orion and Plie (hydraulic and pneumatic damping) and Rheo (MR damping). The results were measured based on quality of life, mobility, satisfaction and injurious falls. Several questionnaires were presented to assess the comfort with the prosthesis and frequency of injurious falls. A significant difference was not observed for functional mobility and satisfaction. In the case of quality of life, differences existed for C-Leg versus Plie, and for injurious falls, in comparison with nonmicroprocessor-based prostheses, C-Leg and Orion performed better, but with aging, C-Leg and Plie performed poorly. The authors in [51] developed an ankle foot orthosis for healthy subjects with MR fluid, as shown in Fig. 12, with an electromagnetic coil, and a spring, which is a combination of semiactive and passive devices. The braking action is achieved by microprocessor-based control that depends on the insole force sensor and ankle angle potentiometer sensor states. The proposed device weighs 819 g and can provide braking during initial foot contact and better dorsiflexion assistance compared to an oil-based damper by avoiding toe drag. However, the authors have also put forth some future modifications in the design process of MR fluid to achieve more output power to implement on gait-disabled patients.

The revolution of active and semiactive orthotic and prosthetic devices has significantly impacted the field of assistive technology, offering improved functionality, comfort, and mobility for individuals with physical disabilities. Active orthotic and prosthetic devices incorporate powered components, such as motors and actuators, to enhance their functionality. Powered prosthetic limbs, exoskeletons, and active ankle-foot orthoses are examples of devices that offer active damping. Some of the advantages of active devices are enhanced functionality and natural movement replication, customizable control and adaptability to various activities, improved energy efficiency and reduced effort for users. However, they have a complex design and higher costs than passive devices. Additional weight and bulkiness due to the

inclusion of motors and power sources, higher power requirements and limited battery life cause slight hinderance for patients. Semiactive orthotic and prosthetic devices combine passive mechanical elements with active components to provide adjustable support and control. Some of the semiactive devices are variable damping systems, sensor-driven control systems, smart materials and actuators. They provide adaptive support and control and personalized assistance because of their ability to dynamically adapt to changing conditions, thus enhancing user safety and ensuring optimal functionality. However, these devices are complex and costlier than passive devices. Additional weight and power requirements due to active components, calibration and maintenance requirements for sensors and control systems are other factors that create setbacks. However, semiactive damping has gained steady pace in the recent decade, which is achieved by electrorheological and magnetorheological fluids. Hence, to achieve good, quick tracking of the knee angle trajectory or better damping at the lower limb joints, variable dampers are preferred over passive fixed damping devices. Variable dampers with smart fluids are light and portable and consume less power than active dampers with pneumatic and hydraulic dampers. Additionally, modelling plays a pivotal role while simulating the real-time systems to envisage the performance of the control strategies. The selection and placement of sensors are important for deciding data capturing parameters such as sampling rate, noise, and bandwidth. The control schemes are sensitive to the type, state, and sampling rate of sensor data for providing appropriate damping in lower limb joints. Hence, the evolution of modelling, sensor selection, and controllers employed in rehabilitative devices are discussed in further sections of the paper.

II. MODELING OF THE KNEE JOINT AND MR DAMPER

The modelling of a system is required to visualize the behavior of the system and to analyse the input and output relationship. The models need to accurately present the linearities and nonlinearities in the system to achieve quality control. In this section, some of the major modelling techniques have been discussed for knee joints and MR dampers using various methods, such as Lagrangian equations, Newtonian equations, multibody modelling, the Bingham model, the Bouc-Wen model and finite element analysis methods.

A. HUMAN KNEE JOINT MODELING

The knee joint models using Newtonian and Lagrangian motion equations shown in Fig. 13 and the neural network were compared, and the estimation of knee torque was carried out in [52]. The former models required anthropometric data captured from motion capture systems, which vary from person to person, whereas the proposed feedforward neural network required data from force sensors. As mentioned in this literature, the learning methods in neural networks provide robust estimation with a normalized root mean square

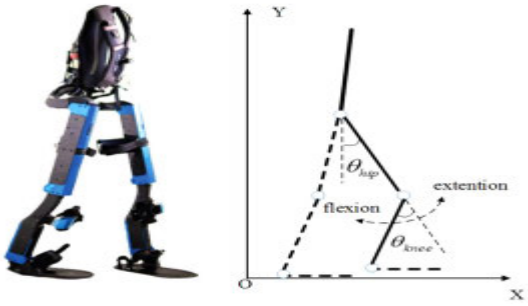

FIGURE 14. Realization of Human lower limbs [53].

error of 2.67% with two kinematic inputs and one kinetic input.

In [53], the model-free adaptive control (MFAC), sliding mode control and prior torque calculator are elaborated, which are responsible for control of the exoskeleton. A weight is assigned to vary the effect of prior torque on the exoskeleton. Referring to Fig. 14, the knee exoskeleton is modelled using the Lagrangian equations given in (1), where M is the inertia matrix (kgmm^2), C is the centripetal and Coriolis matrix, G is the gravitational torque vector (Nmm), τ is the actuator torque vector (Nmm) and τ_h is the torque acting on the exoskeleton (Nmm). The input of the exoskeleton model is torque, and the output is knee joint angle. The knee angle data were obtained from the Vicon motion capture system from a 25-year-old female subject. The simulation is carried out in MATLAB (for visualizing control) and ADAMS (for input and output visualization) software. The hip, knee and ankle errors between the desired and simulated angles are 2.03%, 1.63% and 3.6%, respectively, with a root mean square error of 0.094, thus proving that the proposed method replicates human gait.

$$M(\theta)\ddot{\theta} + C\left(\theta, \dot{\theta}\right)\dot{\theta} + G(\theta) = \tau + \tau_h \tag{1}$$

A demonstration of multibody modelling is carried out in [54] via Simscape to obtain a knee model since rigid bodies (femur, tibia and patella) are interconnected and their motion and interactions in different coordinates are to be analysed. Two joints connecting femur to tibia and patella to femur are modelled to visualize flexion. The joints contain a spring damper that describes stiffness k (Nmm/rad) and damping D (kg/s), and the force f is a resultant (N) when x is the distance between connected bodies given (mm) in (2) referring to Fig. 15 as given in the paper. In this work, authors have compared the Simscape model with Adams model that has been developed for knee of a 77-year-old man. The output of the simulation is flexion and extension of the knee or the angle between the femur and tibia. The proposed model output shows that the absence of ligaments in the model causes missing dynamics; thus, increasing the degree of freedom by including ligaments can provide a more precise model.

$$f = k(x - 1) + D\dot{x} \tag{2}$$

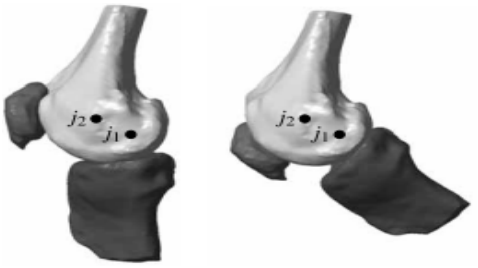

FIGURE 15. Knee joint initial and flexed state [54].

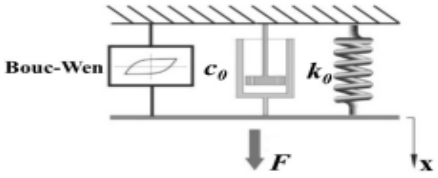

FIGURE 16. Bouc-Wen model of MR damper [55].

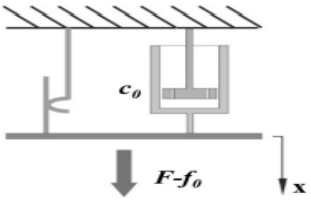

FIGURE 17. Bingham model of MR damper [55].

B. MR DAMPER MODELING

In [55], the properties of MR fluid yield stress, operating temperature range, shear rate, viscosity, density and saturation magnetization are discussed. Models of MR dampers are classified based on the type of modelling. The types are quasistatic (Bingham plastic) and dynamic parametric (Bouc-Wen, Dahl, LuGre), as shown in Figs. 16, 17, and (3)-(4). Dynamic nonparametric (Neural, Fuzzy, Black-box) and inverse dynamic models (Feedforward and recurrent neural network) are explained in [56], [57], and [58]. In these articles, testing of the MR damper to assess the input–output relationship is performed.

$$F = c_0\dot{x} + k_0 x + \alpha z \tag{3}$$

where c_0 is the viscous coefficient (kg/mm/s), k_0 is the stiffness coefficient (N/m) and z is the evolutionary variable.

$$F = f_c sgn\,(\dot{x}) + c_0\dot{x} + f_0 \tag{4}$$

where x is the external solicitation (mm), f_c is the frictional force (N), f_0 is the force offset (N) and c_0 is the damping coefficient (kg/s). In [57], the genetic algorithm is used to analyse the hysteresis behaviour in the Bouc-Wen model of a commercial MR damper. The author has mentioned that under damping, critical damping or over damping of the system dependant on the damper that can be changed by varying the current supplied to the MR damper ranging from 0-1.5 The MR damper is applied to a heavy vehicle seat suspension system with various input vibrations and visualized in the MATLAB environment.

Similarly, in [59], the authors realized the twin rod MR damper MRF-132DG using the Bouc-Wen model, whose parameters are optimized by a genetic algorithm and validated against a standard dataset from experimentation. The inverse model is then integrated with a single-axis two-segment knee model with a forward dynamic MR damper model. A proportional-derivative (PD) plus computed torque control algorithm is incorporated with the prosthesis model and is analysed in MATLAB.

The Bouc-Wen model and experimental data are compared for various frequencies ranging from 0.5-1 Hz with varying currents ranging from 0-1.2 The controller is efficient in minimizing the error between the desired and reference torques. The maximum flexion at the knee during the swing phase with a terminal velocity of 0.44 rad/s can be damped by the MR brake, thus validating the proposed algorithm. In [60], a single-axis MR damper in an above-knee prosthesis is used since damping action is required in the swing phase of the gait cycle. The Bingham plastic model of the MR damper is modelled, and the model parameters are optimized using the Nelder–Mead algorithm. Using finite element analysis, the MR damper characteristics are analysed. In the article, it is proven that the swing trajectory is being followed efficiently. After optimization for a 1 A current, the damper weight was reduced by 71% when compared with the RD-8040-1 damper.

Dynamic models are preferred for the assessment of seismic engineering and automotive applications for vibration attenuation. Furthermore, measurement of MR damper parameters can be challenging in the presence of nonlinearities such as drift, electrical and mechanical noise in sensors, and backlash. The electromagnetic circuit model of the MR damper was validated by comparing the MATLAB simulation with ANSYS [61], [62], [63]. The direct current (DC) and pulse width modulated (PWM) actuation signals were used to excite the MR damper to assess the effect of hysteresis on output power and torque [62], which is depicted in Fig. 18. As mentioned in the literature, by using the PWM actuating signal, the power consumed was 6 W, which is 40% less than the DC signal. Additionally, the PWM 5 kHz, 60% duty cycle signal could deliver 99.8% of the MR damper torque output, and the hysteresis and self-inductance effect in the core and fluid were responsible for the stable torque output even during the off condition of the PWM signal. In Fig. 18, B is the magnetic field strength (T), τ_y is the variable torque (Nmm) generated in the MR fluid and T is the total torque (Nmm) of the MR damper. In [64], the authors proposed finite element analysis (FEA) and computation fluid dynamics analysis (CFDA) for assessing magnetic and fluid flow behavior, respectively. A coupling function that relates FEA and CFDA to provide the output stress. The short-stroke RD-8040-1 MR damper by Lord Corporation displays nonlinearities such as magnetic saturation, viscoelasticity, friction and air gaps, which when considered while modelling can

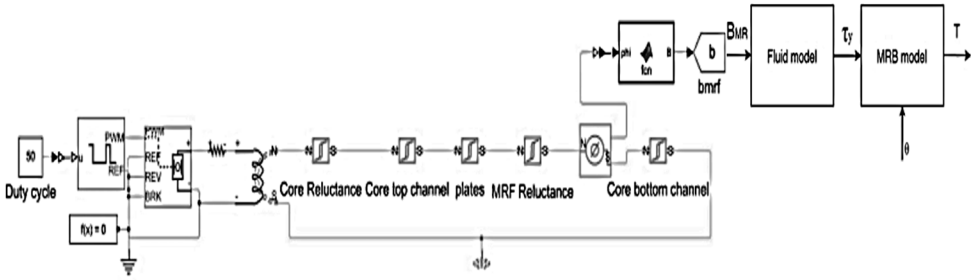

FIGURE 18. PWM used to assess the MR damper model [62].

give better control performance. This section discussed the modelling of knee joints and MR dampers, which is important to have an efficient control algorithm. The Lagrangian and Newtonian equation-based models captured the dynamics of the knee and ankle joints that depended on the equations of motions and energy dissipated at the joints. Multibody modelling can represent the dynamics of limbs if the degrees of freedom are increased. In lower limb modelling, Newtonian modelling focuses on the overall dynamics and kinematics of the limb by simplifying the lower limb as a rigid body system and considers the external forces and moments acting on it and provides insights into joint angles, joint torques, and forces during movement. Lagrangian mechanics is based on the principle of virtual work and the concept of generalized coordinates. It provides a more detailed and comprehensive representation of the dynamics and kinetics of a system. It considers the mass distribution, segmental inertia, and muscle activation patterns while enabling analysis of muscle forces, muscle-tendon lengths, joint reaction forces, and joint moments. However, it is more complex and computationally intensive than Newtonian modelling. If some of the dynamics are omitted or simplified in the equations of motion, this might lead to inaccuracy with the actual limb dynamics. While multibody dynamics accurately simulates the dynamic behavior of the lower limb and orthotic devices, it considers the interactions between rigid bodies and joints. This provides insights into joint kinematics, forces, and torques during dynamic activities. It can be computationally demanding, especially for complex systems. The MR damper models using the Bouc-Wen and Dahl-LuGre methods represent the damper using spring-mass-damper systems, and these can show only linearities in the system. To cover the nonlinearities in the MR damper, the genetic algorithm and finite element analysis methods are preferred. For MR damper modelling, the choice between the Bingham model, Bouc-Wen model, FEA, and CFDA depends on the specific requirements of the analysis or design process. The Bingham model is simple but may not capture all the complexities of MR dampers. The Bouc-Wen model provides a more accurate representation of hysteresis. Modified Bouc-Wen model can capture additional dynamics by adding additional terms in the fundamental equation. FEA allows for detailed structural analysis but requires additional constitutive models for the MR fluid. CFDA provides a comprehensive understanding of the fluid flow behavior but requires advanced numerical methods and computational resources. Additionally, accuracy may be influenced by assumptions about fluid behavior and boundary conditions. Finite element analysis (FEA) enables detailed analysis of the mechanical behavior of the fluids by providing insights into stress distribution, deformation, and structural response. It is also useful for optimizing device design and predicting its performance under different loading conditions. However, it requires accurate material properties and boundary conditions for accurate simulations. Additionally, it can be computationally intensive, time-consuming and difficult to validate with real time data. Logic decision trees are interpretable, as they provide explicit rules that lead to specific outcomes. They are relatively easy to implement and understand, making them suitable for simpler lower limb models. Decision trees can handle categorical and continuous input variables, making them versatile for different types of data. However, decision trees may struggle with capturing complex relationships and interactions between variables, especially when the dataset is large and high-dimensional, and are prone to overfitting, especially when the model becomes more complex or when the dataset is small. Neural networks can capture nonlinear relationships and handle high-dimensional data, making them suitable for more complex lower limb models. They can handle a wide range of input and output types, including both categorical and continuous variables. However, neural networks are often considered ''black-box'' models, as they lack interpretability compared to decision trees, require a large amount of training data to generalize well and may be prone to overfitting if the dataset is small. Neural networks are computationally intensive and require more resources for training and inference than decision trees.

III. TYPES OF SENSORS USED IN REHABILITATIVE DEVICES

Various sensors, such as inertial measurement units (IMUs) and flexible sensors, have been used to measure knee angles during different gait phases. Machine learning techniques and heuristic methods require proper data to achieve accurate predictions. Proper selection of sensors is critical based on the signal processing, number of sensors used, placement area,

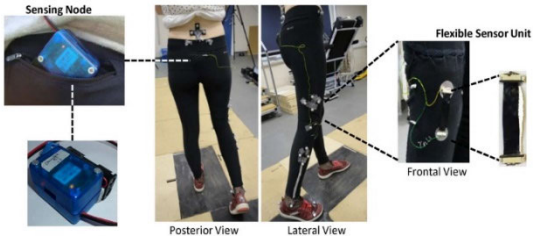

FIGURE 19. Flexible polymer sensor [73].

FIGURE 20. Dielectric elastomer sensor placed on knee [75].

and weight. Some of the sensors used are wearable goniometers [65], piezo electric sensors, microphones [66], [67], mechanical sensors [68], accelerometers [69], [70], wearable gyroscopes, foot pressure sensors [71], strain sensors, smartphone inertial sensors, force sensors [72] and textile capacitive sensors.

A. FLEXIBLE RESISTIVE TYPE SENSORS

In [73], a flexible polymer unit was developed that was stitched to leggings, as shown in Fig. 19, which changed its conductivity based on the stretching of limbs, and data acquisition was wireless. In this work, the voltage outputs were correlated with knee flexion angles during gait. Intraclass correlation coefficients were used to evaluate the test-retest reliability. The proposed sensor system is compared with ten camera motion capture systems. Sixteen participants were chosen for the study for both systems. The absolute error and relative mean square error were 0.35 and 1.2, respectively, and the intraclass correlation coefficient was greater than 0.8, thus proving the ability of the proposed system for knee angle measurement.

Flexible sensors stitched on a garment are placed on the wrist, elbow and knee since more bending movements occur in these joints [74]. The sensor is calibrated by experimenting on various diameters, and a second-order polynomial equation is presented. A 34-year-old male subject with healthy joints is selected to test the flexible smart garment for standing and walking tests. For twenty-two cycles of walking at 4 km/h, sensor sensitivities for wrist, elbow and knee were 0.94°, 0.8° and 0.56°, and the maximum flexion angles were 80°, 95° and 140°, respectively. The ranges of measurement for the wrist, elbow and knee joints were 40-45°, 70-90° and 40-75°, respectively, thus making the sensor a viable option for angle measurement.

FIGURE 21. Flexible goniometer and IMU for knee joint angle measurement [65].

FIGURE 22. Mechanical sensor to measure lower limb joint angles [67].

A flexible dielectric elastomer sensor, a strain measuring device, is used to measure knee angles in the sagittal plane [75], as shown in Fig. 20. The sensor working is realized using an equivalent circuit with strain as the input and output being the voltage. The sensor is stitched on the pants for hip and knee joint angle measurement, as shown in Fig. 20. The circuit model of the strain sensor is validated against an actual model by experimentation. On comparison with motion capture system Phasespace, at different walking speeds, the proposed sensor is found to be comparable and feasible with squatting and walking detection at 3° and 5° accuracy, respectively, with a sampling frequency of 200 Hz.

B. MECHANICAL SENSORS

In [65], the authors developed a piezo-electric electromechanical goniometer that measures knee flexion and extension. The two layers of piezoelectric materials are isolated via an insulating layer between them. The change in the extent of bending results in a change in the resistance of the material. Additionally, inertial measurement unit (IMU) sensors are fused along with a goniometer, as shown in Fig. 21, using the Kalman filtering technique to estimate the overall angle of the knee joint.

In [68], a mechanical measuring device was developed, as depicted in Fig. 22. The device is placed on the limbs where there is a change in the angle of the limbs, such as on the hip, knee and ankle joints. The measurement card placed in the holder resembles a protractor, and the pointer moves along the measurement as and when the limb moves. This is helpful

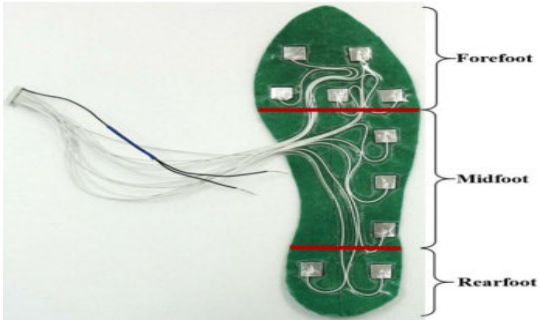

FIGURE 23. Electrodes placed on the insole of shoe [76].

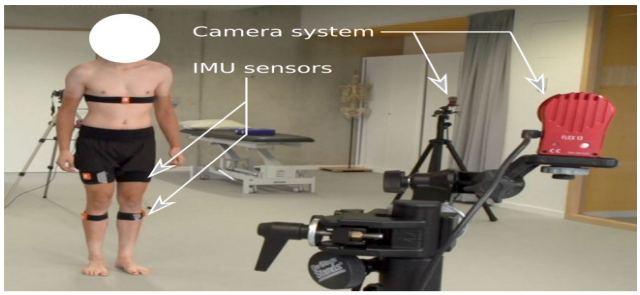

FIGURE 24. Placement of IMU on limb [78].

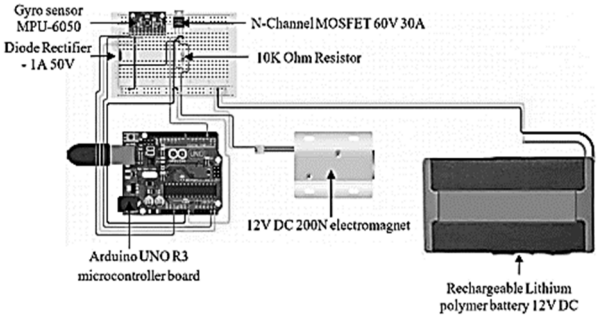

FIGURE 25. Gyro sensor to measure the knee joint angle [82].

FIGURE 26. Combination of acoustic sensors [66].

in the dynamic measurement of angles (flexion/extension) of lower limb joints. Fig. 23 illustrates the use of capacitive textile sensors in [76] to measure the pressure under the foot. Capacitive sensors are placed on the inner sole that change the capacitance based on the force applied by the foot during various phases of gait or movements [77]. An artificial neural network is used to predict the angles of the lower limb based on the data obtained from capacitive sensors placed in three different shoes with normal and fast gait patterns.

C. BODY-ORIENTATION BASED SENSORS

The authors in [78] used IMU sensors placed arbitrarily on the limbs with sensor frames aligned with the vertical gravity axis to record knee angles, as depicted in Fig. 24. The sensor data are conditioned to obtain angular velocity and linear accelerations using accelerometers and gyroscopes [79], [80]. The orientation and position of knee axes in reference frames is achieved by minimizing the cost function. A smoothing filter depends on the dynamic model of the legs to estimate the leg segment motion. In this paper, the proposed algorithm is tested on a robotic leg and compared with a motion capture system for lunge movement. The results indicate that the proposed method is able to estimate varus and valgus muscle movement and internal and external rotation within a feasible range of motion.

In [81], commercially available Runscribe sensors were used to measure step count and cadence, which are wearable accelerometer and gyroscope-based sensors, and heart rate was obtained from a Polar T-31 chest strap and FT1 watch. Fifteen participants (ages 17 to 23) were involved in the study, which was carried out for three days and made to run for 1600 m on track and grass surfaces. The Runscribe sensors were able to detect the differences in running speeds and on surfaces, and the results were comparable with motion capture systems. Similarly, an electromagnet-based knee locking mechanism is proposed, and the prototype geared the knee with a gyroscope-based sensor [82]. The electromagnet is controlled by an atmega (AVR family) microcontroller for the locking mechanism based on the thigh position provided by the gyro sensor, as shown in Fig. 25.

The proposed method is tested experimentally by applying disturbances to visualize the locking mechanism, thus preventing the patient from falling. The device is capable of recreating the healthy limb gait and creates a locking mechanism for sudden inputs.

D. MULTIMEASUREMENT SENSORS

The authors in [66] developed an integrated knee angle measuring system. The piezo electric film is accompanied by two airborne microphones, i.e., the commercially available electret and micro electromechanical system (MEMS), which are used to measure the acoustic emissions from knee joints. From the acoustic signals, it is found that the type of emissions is particular for all the movements of knee joints. Additionally, IMUs were placed above the knee and on the shank to measure the change in the angles of the lower limbs,

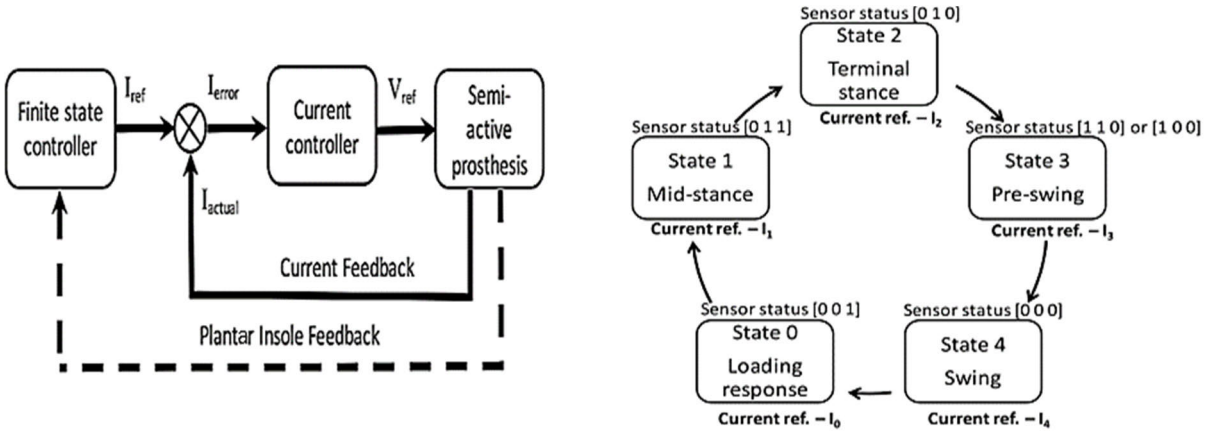

FIGURE 27. Control flow diagram for prosthesis [77].

as shown in Fig. 26. Flexible sensors such as polymer-based, piezoelectric, and capacitive sensors are able to provide electrical output based on the bending of the knee and ankle joints. There is less necessity of processing data in these types of sensors, unlike inertial sensors, where filtering needs to occur every now and then eliminate the accumulation of errors. In summary, strain gauge sensors are highly accurate for measuring localized forces, while they require careful mounting and calibration for accurate measurements. Piezoelectric sensors provide a fast response and high sensitivity, are susceptible to temperature variations and can exhibit hysteresis. IMU combines accelerometers, gyroscopes, and sometimes magnetometers may suffer from drift over time and require calibration. Mechanical Goniometers provide direct measurement of joint angles and are relatively simple and low-cost. However, they are limited to specific joint measurements and may restrict motion. Flexible goniometers are lightweight, flexible, and conformable to the body and can be integrated into wearable devices but are prone to hysteresis and drift over time. Acoustic sensors are noninvasive and provide real-time data but can be affected by background noise and require signal processing techniques [94].

In conclusion, multimeasurement sensors and mechanical sensors tend to offer higher accuracy and precision compared to flexible resistive type and body-orientation based sensors. Multimeasurement sensors can capture a wide range of data, including movement, orientation, and forces. Mechanical sensors are limited to specific types of motion. Flexible resistive type sensors are often more comfortable to wear due to their flexibility and conformability. Body-orientation based sensors and IMUs are compact and suitable for wearable devices. Body-orientation based sensors and multimeasurement sensors (IMUs) provide real-time monitoring of movement and orientation, making them suitable for dynamic activities. mFlexible resistive type sensors are relatively cost-effective and simple to implement. Multimeasurement sensors can be more expensive and require advanced signal processing and calibration. Mechanical sensors are generally durable and reliable due to their direct mechanical measurement. Body-orientation based sensors may require protection from external impacts. Flexible resistive type sensors are often used for simple joint angle measurement and pressure distribution analysis. Mechanical sensors find applications in joint angle measurement. Body-orientation based sensors and multimeasurement sensors are suitable for gait analysis, posture monitoring, and more complex movement assessment.

IV. CONTROL ALGORITHMS IN REHABILITATIVE DEVICES

To achieve the required braking at the knee/ankle joints during different phases of the gait cycle, the control algorithm must provide quick and efficient output [83], [84]. The control schemes discussed, such as finite state machine, machine learning, fuzzy control, sliding mode control and hybrid control, such as fuzzy-PID, provide damping based on inputs such as sensor states or trajectory states.

A. FINITE STATE MACHINE AND MACHINE LEARNING CONTROL

In [85], an MR damper-based prosthetic mechanical leg was developed. The gait phases were detected by the inertial measurement unit comprising an accelerometer, gyroscope and magnetometer, whereas the angular velocity was measured by an encoder. These sensors are embedded in a Teensy microcontroller, which also serves as a platform for communication via a wireless Xbee module. The MR damper is controlled by the pulse width modulation (PWM) of the microcontroller. Finite state machine-based control has been proposed for smooth transitioning from heel strike (HS), foot flat (FF), toe off (TO) and mid swing (MSW) phases of gait based on the sensor state z_i. An identification procedure was carried out using reflective markers of the motion capture system, and for normal walking speed, the HS, TO and MSW phases were successfully identified.

According to [77], two controllers, a finite state machine for providing reference current based on insole foot sensor output and a proportional-integral (PI) controller (receiving Hall sensor output from the MR damper), as shown in Fig. 27, for achieving desired braking from the MR damper

are essential for efficient control. A 24-year-old male transfemoral amputee who had been using a passive prosthesis for three years was taken as the subject for this study. The prosthesis weighed 1.77 kg and cost 22,000 INR. The device was able to deliver normal gait for swing and stance phases with constrained movement at approximately 70°. The average power consumption of the prosthesis is 2.25 W with a battery of 9 V and 2.4 AHr for the gait cycle on ground level walking and requires charging once a day.

Ankle position and electromyography signals were the two inputs that provided datasets for training the nonlinear autoregressive exogenous neural network [86], as shown in Fig. 28. The damping stiffness is the output of the MR damper of the orthosis and depends on the output of the neural network. The proposed optimization algorithm reduced the number of sensors, i.e., only ankle sensor data were considered, thus reducing the weight of the orthosis. Additionally, the Bayesian regularization training algorithm was best suited when compared with other training algorithms, with fifteen hidden layers and a delay of 2 and a mean squared error and coefficient of determination of 19.16 and 0.992, respectively. In [87], various sensors such as mechanomyogram (MMG), EMG, IMU, strain gauge, and force sensors as inputs to neural networks are discussed. The control algorithms based on neural networks (predefined trajectory tracking and gait-pattern, human–machine interaction based, adaptive oscillator based, neuromuscular model-based control) are discussed. The author of [87] proposed a template-based force modulated compliant ankle (FMCA) that used ground reaction forces as variables in ankle prostheses for angle control using a finite state machine, as shown in Fig. 29. The simulation of the proposed algorithm was compared with experimental data, and the results were feasible for real-time application. The proposed control algorithm was adopted for a powered orthosis on a treadmill with twenty-one healthy subjects. The vertical ground reaction force (GRF) values, ankle angle and torque during assisted walking were comparable to those during normal walking. The footswitch sensor and EMG sensors were used to measure various angles and muscle activities during walking [88], as shown in Fig. 30. The features were extracted and fed to the neural network, where the Levenberg–Marquardt (LM) and scaled conjugate gradient (SCG) neural network algorithm efficiency was compared to control braking using an MR damper.

The number of feature inputs to the neural network was also of concern. Three participants aged 22-25 were chosen for the study and were asked to walk on the treadmill for one minute. On training the neural network algorithms ten times with 2, 10, 12 and 14 features, the Levenberg–Marquardt algorithm performed better by 2% than the SCG algorithm in terms of the average classification rate. The neural network accuracy increased by 5% when at least or more than ten inputs were used instead of two inputs. In [89] and [90], surface EMG signals were used in a prosthetic arm to assess muscular electrical activity. The authors of [89] used Myo armband at triceps and biceps of the amputated arm. Ten time-domain features were selected for the classifier to detect motions of the arm. Fifteen healthy and four amputated individuals were chosen for the study, and arm motions, namely, elbow extension and flexion, wrist pronation and supination, were evaluated using surface EMG signals. The signal mean and waveform length were the best feature combination, and with the classification algorithm as k-nearest neighbours, the simulation accuracy was 95.8% and 68.1%, and the real-time accuracy was 91.9% and 60.1% for healthy subjects and amputees, respectively.

The authors in [91] proposed an MR damper forward mechanical model based on the sigmoid method and using back propagation neural network, and an inverse model is also proposed. To address model uncertainties, a second-order sliding mode controller is designed [86], [87]. For level walking, the proposed prosthesis is compared with the normal gait (Lagrangian model) trajectory. The maximum error for the swing trajectory is 9.4%, thus validating the method.

Strain gauge sensors and angle sensors are used to measure the amount of deformation in carbon foot and ankle rotation [88], respectively.The data from the strain gauge sensor are fed to a five-layer convolution neural network for training and gait recognition. Three transtibial amputees were chosen as subjects and performed 35 cycles of walking, climbing up and down the ramp and stairs. The overall three-mode gait recognition was 92.06±1.34% for the hold-out test and 92.53±1.61% for 5-fold cross-validation. From the literature review, it is found that orthoses play a major role in resuscitating limb movements by providing additional assistance to limbs. In [89], **an** MR damper is realized as a double pendulum model obtained by using Lagrangian equations. The reward shaping method in Q-learning control is adopted for the control of braking in the MR damper for swing phase trajectory tracking. The simulation is carried out using an Intel processor. The dataset used for simulation is gathered from a male weighing 87 kg and 1.75 m tall who is made to walk on a treadmill at different speeds (2.4, 3.6 and 5.5 km/h). The proposed model is compared with the previous work carried out by the same authors. In comparison with another adaptive dynamic programming (ADP) algorithm, the average RMSE of the proposed prosthetic knee is 1.59° and that of the ADP-based knee is 2.5°. The knee angle sensor (on the thigh connector), IMU (on the shank), and load cell force sensor (embedded in the shank) were used to measure the extension and flexion angles of the knee joint [90], as depicted in Fig. 31. The microprocessor controller has a state machine for the detection of gait phases that controls the electrically actuated hydraulic damper to achieve braking. The prototype is tested on a robotic walking ground simulator. The experiment was carried out on a treadmill (45 gait cycles) for different walking speeds (0.6 m/s, 1.1 m/s and 1.6 m/s) to check speed adaptation, gait phase recognition and symmetry [95]. The kinematics were obtained by a motion capture system. The prosthetic knee symmetry is compared with the simulated normal foot, and via a symmetry index, it is concluded that

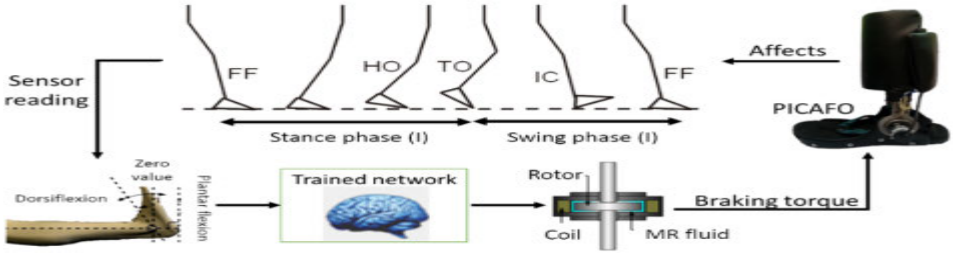

FIGURE 28. Intelligent control algorithm for Ankle foot orthosis [82].

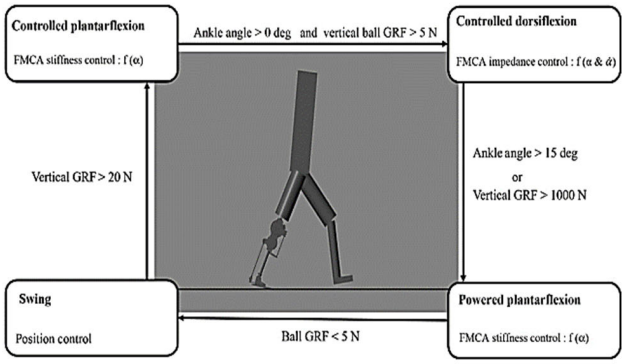

FIGURE 29. Control algorithm depending on sensor states [87].

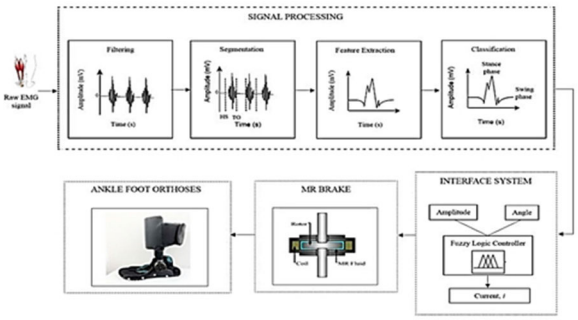

FIGURE 30. Control process depending on EMG sensor [83].

the proposed algorithm is acceptable (98.8% for 0.6 m/s, 98% for 1.1 m/s and 96.4% for 1.6 m/s). In [96], a dataset for a logic decision tree was obtained from thirty healthy individuals. Ten strides with knee angles, thigh angular velocity and acceleration features are used in MATLAB and interpolated for 200 Hz. The data are obtained for different walking speeds and conditions. Additionally, another set of data was obtained from twelve healthy participants for validation. A correction algorithm called transition sequence verification and correction is used to improve the results from the logic decision tree, as shown in Fig. 32. The gait phase features, such as loading response, push-off, swing and terminal swing, were compared with the validation set and proposed algorithm both before and after using the correction algorithm. The accuracy increased to 98.72% from 98.38% for the first training set and 60% to 98.61% for the validation set. The sensitivity and F score indicated the feasibility of the proposed algorithm for application in ankle orthosis.

B. HYBRID CONTROL

An intelligent above-knee prosthesis [97] was proposed by the authors. A four-bar link mechanism was employed to visualize the knee joint. The MR damper acts as the meniscus of the actual human knee and provides shock absorption during tenuous activities. The forward Bouc-Wen model and inverse neural network models are designed and analysed in ANSYS software to visualize the input current and output damping variables. To accommodate the drawbacks of PID control, since the MR damper is nonlinear, fuzzy PID control is designed based on trajectory tracking to control the current to the MR damper, thus providing the desired braking, and the results are proven to be satisfactory with minimum error. The MR damper is tested experimentally to obtain a spring-mass-damper model of the same [98], [99]. Proportional-integral-derivative (PID) control and fuzzy PID control are applied to the MR damper-knee prosthesis model, as shown in Fig. 33, and the performance is compared. The inclusion of a semiactive MR damper gives variable damping rather than passive damping to protect the limb from further injury. The proposed fuzzy PID controller provides better damping and shock absorption than PID control.

The finite state control scheme is dependent on the state of the sensors employed in the rehabilitative devices. It is considered an efficient control algorithm since the finite states can be defined priorly to achieve good control. Whereas conventional PID control may fail if there are nonlinearities such as hysteresis, backlash and saturation, hybrid control strategies such as fuzzy-PID are employed to cover the negative effects before they affect the system. Additionally, neural networks are computational models that excel at handling high-dimensional data, capturing nonlinear relationships, and adapting to dynamic environments, as discussed earlier. Fuzzy control is used to handle uncertainties, variability, and nonlinearity in the control system. Fuzzy control is particularly suitable when there are complex and ambiguous relationships between input and output variables. It provides robustness against noise and uncertainties in the system and can handle nonlinear dynamics effectively. However, fuzzy

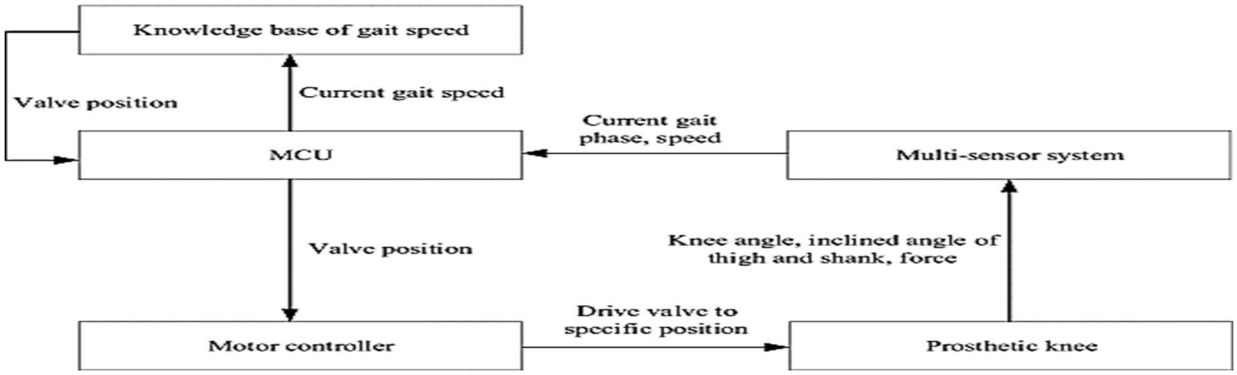

FIGURE 31. Control algorithm for prosthetic knee [90].

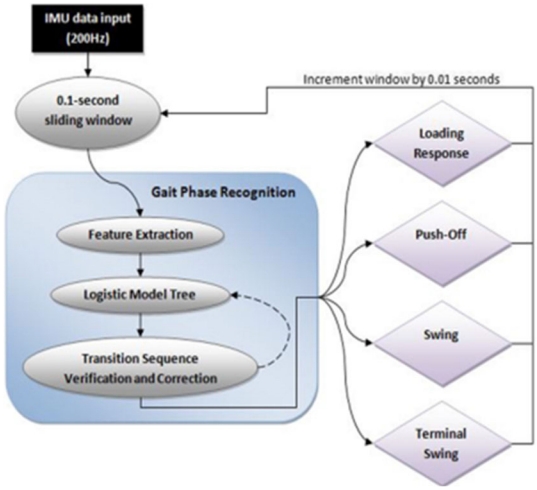

FIGURE 32. Gait phase control with IMU data input [96].

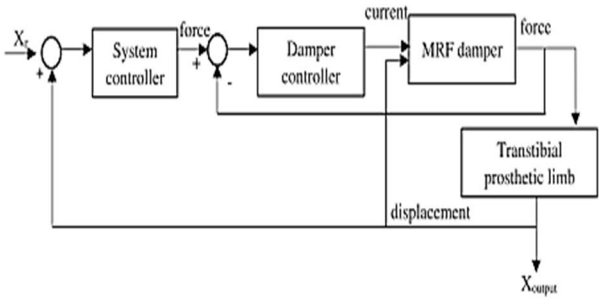

FIGURE 33. Control diagram for transtibial prosthetic limb [98].

control may require manual rule design and tuning, which can be time-consuming and subjective. Q-learning is used for adaptive and autonomous control by enabling devices to learn optimal control policies through trial and error and interaction with the environment. It can handle complex and dynamic systems, allowing devices to adapt to changing conditions and providing adaptive and personalized assistance based on user preferences and feedback [100]. However, Q-learning typically requires a large number of iterations to converge and may suffer from the curse of dimensionality in high-dimensional state-action spaces. Hybrid fuzzy-PID control integrates the flexibility and adaptability of fuzzy logic with the precise control and stability of PID control. It allows for intelligent decision-making based on fuzzy rules while incorporating PID control for fine-tuning and stability. However, designing and tuning the hybrid fuzzy-PID control system may require expertise and careful parameter adjustment. In summary, FSM has limited adaptability and predefined states may not cover all user scenarios. Whereas ML based control has high adaptability and learns from data and can handle a wide range of scenarios. Hybrid control has balanced adaptability, leverages ML for user-specific adaptations while maintaining structured control. FSM requires no learning by relying on predefined rules while ML requires training with relevant data to adapt over time. Hybrid control combines predefined rules with adaptive learning. FSM has clear control logic and safety features can be integrated. In ML based control safety may be a concern due to potential unpredictable behavior. Hybrid control combines structured safety mechanisms with adaptive learning. FSM has a relatively simple design and implementation but ML based control can be complex due to data collection, model training, and validation. In Hybrid control, complexity lies in integrating different control components effectively. FSM has fast real-time response by transitioning between predefined states quickly, meanwhile ML based control response time may be affected by computation and training requirements. In Hybrid control, response time depends on the combination of control modes.

V. CONCLUSION

This paper provides an overview of the importance of rehabilitative devices, the evolution of orthoses with regard to sensors used in prosthetic and orthotic devices, the modelling of knee joints and MR dampers, and the control algorithms used in rehabilitative devices. Orthoses are essential when patients have limb-related muscular disorders, neural disorders, minor injuries, and ankle movement assistance, and prostheses are required in cases of amputation of the knee

or ankle. The rehabilitative devices have evolved over the years starting with the basic fabric type or fixed damping type and moved on to variable damping with hydraulic, pneumatic actuators initially, tethered and bulky, later switching on to portable. Modelling is pivotal when efficient control is necessary, and in the case of orthosis/prosthesis control, the human limb requires quicker control to achieve the required damping within a few milliseconds. The modelling techniques of MR dampers and lower limbs have evolved from mathematical equations of motion such as Bingham, Bouc Wen, Lagrangian, and Newtonian to intelligent modelling techniques such as logic decision trees and neural networks that incorporate nonlinearities. A variety of sensors have been utilized to capture accurate data to achieve better control of smart rehabilitative devices. Sensors such as EMG, strain gauge sensors, piezoelectric sensors, IMU, mechanical goniometers, flexible goniometers, and acoustic sensors have been used widely over the years, and the placement area of these sensors plays a vital role in recording data. Overall, the choice of sensor depends on the specific application requirements, desired measurements, and device's intended use. Each sensor has advantages and limitations in terms of accuracy, reliability, sensitivity, ease of use, and cost. Integrating multiple sensors and employing sensor fusion techniques can often enhance the overall performance and robustness of orthotic and prosthetic devices. The sampling rate of the data collection also plays an important role in the response time of the overall control system and data preservation. The control algorithms discussed in this paper range from basic PID control, which has difficulty handling nonlinearities, to advanced control algorithms such as neural networks, fuzzy control, Q-learning, and hybrid fuzzy-PID control to compensate for the effects of inherent or external nonlinearities. The choice between neural networks, fuzzy control, Q-learning, and hybrid fuzzy-PID control depends on the specific requirements of the orthotic and prosthetic device, the complexity of the control problem, the availability of training data, and the desired trade-off between interpretability, adaptability, and control performance. It is important to evaluate the strengths of each method and limitations in the context of the specific application to determine the most suitable approach.

VI. FUTURE SCOPE

The field of active and semiactive orthotic and prosthetic devices holds significant potential for future advancements.

The development of more sophisticated control systems is a key area of future research. This includes the integration of machine learning and artificial intelligence techniques to enhance device performance and adaptability. These advanced control systems can learn from user interactions, optimize device behavior, and provide personalized assistance based on individual needs and preferences. The future of active and semiactive devices involves miniaturizing components such as motors, sensors, and power sources to reduce the overall size and weight of the devices. This will enhance user comfort and acceptance, allowing for more seamless integration into everyday life. The incorporation of wireless communication technologies can enable seamless connectivity between the device, sensors, and control systems. This facilitates real-time data transmission, remote monitoring, and updates, enhancing the device's functionality and enabling healthcare professionals to remotely assess and adjust device parameters. Future developments may focus on harnessing and storing energy from the user's movements to power the devices. Energy harvesting technologies, such as kinetic energy or heat harvesting, can reduce the reliance on external power sources and increase the device's autonomy. Providing users with sensory feedback, such as pressure or vibration, can enhance their proprioception and improve the naturalness of device usage. Future devices may incorporate haptic interfaces or feedback systems that simulate the sensation of touch and enhance the user's awareness of their environment and device interaction. Advancements in biomechanical modelling and simulation can enable the optimization of device parameters based on individual user characteristics. Virtual modelling and analysis can help tailor the devices to specific biomechanical needs, improving overall device performance and user satisfaction. Future devices will likely prioritize user-centric design, considering individual preferences, body morphology, and functional requirements. Customization through 3D printing and rapid prototyping techniques will become more accessible, allowing for personalized device fitting and improved user comfort. The development of more advanced and accurate sensors will provide improved feedback and enable a deeper understanding of user movements and intent. This can lead to more precise control algorithms and assistive strategies, resulting in devices that seamlessly integrate with the user's biomechanics and provide more natural and intuitive assistance. The future of active and semiactive orthotic and prosthetic devices holds great promise for improving the quality of life for individuals with physical disabilities. These advancements aim to provide greater functionality, comfort, and adaptability, allowing users to regain mobility and independence. Ongoing research and technological innovations will continue to shape the future of these devices, paving the way for more advanced and personalized assistive technologies.

CONFLICTS OF INTEREST

The authors declare that there is no conflict of interest regarding the publication of this article''.

REFERENCES

[1] Tradusway. *What Are Knee Braces?* Accessed: Apr. 4, 2022. [Online]. Available: https://www.slideshare.net/Tradusway12/what-are-knee-braces

[2] J. B. Ring and C. Kim, "A passive brace to improve activities of daily living utilizing compliant parallel mechanisms," in *Proc. 40th Mech. Robot. Conf.*, Aug. 2016, pp. 1–10, doi: 10.1115/DETC2016-59616.

[3] W. Lovegreen and A. B. Pai, "Orthoses for the muscle disease patient," in *Orthoses for the Muscle Disease Patient*, 4th ed. Amsterdam, The Netherlands: Elsevier, 2019, pp. 332–336, doi: 10.1016/b978-0-323-48323-0.00032-9.

[4] K. Mills, P. Blanch, A. R. Chapman, T. G. McPoil, and B. Vicenzino, "Foot orthoses and gait: A systematic review and meta-analysis of literature pertaining to potential mechanisms," *Brit. J. Sports Med.*, vol. 44, no. 14, pp. 1035–1046, Nov. 2010, doi: 10.1136/bjsm.2009.066977.

[5] M. Sliepen, E. Mauricio, and D. Rosenbaum, "Acute and mid-term (six-week) effects of an ankle-foot-orthosis on biomechanical parameters, clinical outcomes and physical activity in knee osteoarthritis patients with varus malalignment," *Gait Posture*, vol. 62, pp. 297–302, May 2018, doi: 10.1016/j.gaitpost.2018.03.034.

[6] J. Mo and R. Priefer, "Medical devices for tremor suppression: Current status and future directions," *Biosensors*, vol. 11, no. 4, p. 99, Mar. 2021, doi: 10.3390/bios11040099.

[7] J. W. Ng, L. J. Y. Chong, J. W. Pan, W.-K. Lam, M. Ho, and P. W. Kong, "Effects of foot orthosis on ground reaction forces and perception during short sprints in flat-footed athletes," *Res. Sports Med.*, vol. 29, no. 1, pp. 43–55, Jan. 2021, doi: 10.1080/15438627.2020.1755673.

[8] L.-F. Yeung, C. Ockenfeld, M.-K. Pang, H.-W. Wai, O.-Y. Soo, S.-W. Li, and K.-Y. Tong, "Randomized controlled trial of robot-assisted gait training with dorsiflexion assistance on chronic stroke patients wearing ankle-foot-orthosis," *J. NeuroEng. Rehabil.*, vol. 15, no. 1, pp. 1–12, Dec. 2018, doi: 10.1186/s12984-018-0394-7.

[9] B. Chen, B. Zi, Z. Wang, L. Qin, and W.-H. Liao, "Knee exoskeletons for gait rehabilitation and human performance augmentation: A state-of-the-art," *Mechanism Mach. Theory*, vol. 134, pp. 499–511, Apr. 2019, doi: 10.1016/j.mechmachtheory.2019.01.016.

[10] H. Akuzawa, A. Imai, S. Iizuka, N. Matsunaga, and K. Kaneoka, "Tibialis posterior muscle activity alteration with foot orthosis insertion measured by fine-wire electromyography," *Footwear Sci.*, vol. 13, no. 2, pp. 157–165, May 2021, doi: 10.1080/19424280.2021.1893835.

[11] S. T. Kwee-Meier, A. Mertens, and S. Jeschke, "Age-induced changes in the lower limb muscle activities during uphill walking at steep grades," *Gait Posture*, vol. 62, pp. 490–496, May 2018, doi: 10.1016/j.gaitpost.2018.04.003.

[12] J. Katsuhira, S. Yamamoto, N. Machida, Y. Ohmura, M. Fuchi, M. Ohta, S. Ibayashi, A. Yozu, and K. Matsudaira, "Immediate synergistic effect of a trunk orthosis with joints providing resistive force and an ankle-foot orthosis on hemiplegic gait," *Clin. Interventions Aging*, vol. 13, pp. 211–220, Feb. 2018, doi: 10.2147/CIA.S146881.

[13] K. A. Shorter, G. F. Kogler, E. Loth, W. K. Durfee, and E. T. Hsiao-Wecksler, "A portable powered ankle-foot orthosis for rehabilitation," *J. Rehabil. Res. Dev.*, vol. 48, pp. 459–472, Nov. 2010.

[14] E. T. Hsiao-Wecksler, K. A. Shorter, Y. Li, G. F. Kogler, and W. K. Durfee, "Portable pneumatically-powered ankle-foot orthosis," *J. Med. Devices*, vol. 6, no. 1, p. 17593, Mar. 2012.

[15] M. Arazpour, A. Chitsazan, S. W. Hutchins, F. T. Ghomshe, M. E. Mousavi, E. E. Takamjani, G. Aminian, M. Rahgozar, and M. A. Bani, "Design and simulation of a new powered gait orthosis for paraplegic patients," *Prosthetics Orthotics Int.*, vol. 36, no. 1, pp. 125–130, 2012, doi: 10.1177/0309364611431481.

[16] Y. Bai, X. Gao, J. Zhao, F. Jin, F. Dai, and Y. Lv, "A portable ankle-foot rehabilitation orthosis powered by electric motor," *Open Mech. Eng. J.*, vol. 9, no. 1, pp. 982–991, Oct. 2015.

[17] D. Case, B. Taheri, and E. Richer, "Active control of MR wearable robotic orthosis for pathological tremor suppression," in *Proc. Dyn. Syst. Control Conf.*, Oct. 2015, pp. 1–8, doi: 10.1115/DSCC2015-9874.

[18] H. S. Nguyen and T. P. Luu, "Tremor-suppression orthoses for the upper limb: Current developments and future challenges," *Frontiers Hum. Neurosci.*, vol. 15, 2021, Art. no. 622535, doi: 10.3389/fnhum.2021.622535.

[19] Z. Zhang, H. Yu, W. Cao, X. Wang, Q. Meng, and C. Chen, "Design of a semi-active prosthetic knee for transfemoral amputees: Gait symmetry research by simulation," *Appl. Sci.*, vol. 11, no. 12, p. 5328, 2021, doi: 10.3390/app11125328.

[20] Y. Sun, R. Huang, J. Zheng, D. Dong, X. Chen, L. Bai, and W. Ge, "Design and speed-adaptive control of a powered geared five-bar prosthetic knee using BP neural network gait recognition," *Sensors*, vol. 19, no. 21, p. 4662, 2019, doi: 10.3390/s19214662.

[21] E. R. Esposito, K. A. Schmidtbauer, and J. M. Wilken, "Experimental comparisons of passive and powered ankle-foot orthoses in individuals with limb reconstruction," *J. NeuroEng. Rehabil.*, vol. 15, no. 1, pp. 1–10, Dec. 2018, doi: 10.1186/s12984-018-0455-y.

[22] Y. Sun, H. Tang, Y. Tang, J. Zheng, D. Dong, X. Chen, F. Liu, L. Bai, W. Ge, L. Xin, H. Pu, Y. Peng, and J. Luo, "Review of recent progress in robotic knee prosthesis related techniques: Structure, actuation and control," *J. Bionic Eng.*, vol. 18, no. 4, pp. 764–785, Jul. 2021, doi: 10.1007/s42235-021-0065-4.

[23] B. Chen, B. Zi, Y. Zeng, L. Qin, and W.-H. Liao, "Ankle-foot orthoses for rehabilitation and reducing metabolic cost of walking: Possibilities and challenges," *Mechatronics*, vol. 53, pp. 241–250, Aug. 2018, doi: 10.1016/j.mechatronics.2018.06.014.

[24] O. Kirtas, Y. Savas, M. Bayraker, F. Baskaya, H. Basturk, and E. Samur, "Design, implementation, and evaluation of a backstepping control algorithm for an active ankle-foot orthosis," *Control Eng. Pract.*, vol. 106, Jan. 2021, Art. no. 104667, doi: 10.1016/j.conengprac.2020.104667.

[25] F. Giovacchini, F. Vannetti, M. Fantozzi, M. Cempini, M. Cortese, A. Parri, T. Yan, D. Lefeber, and N. Vitiello, "A light-weight active orthosis for hip movement assistance," *Robot. Auto. Syst.*, vol. 73, pp. 123–134, Nov. 2015, doi: 10.1016/j.robot.2014.08.015.

[26] J. Narayan, B. Kalita, and S. K. Dwivedy, "Development of robot-based upper limb devices for rehabilitation purposes: A systematic review," *Augmented Human Res.*, vol. 6, no. 1, pp. 1–33, Dec. 2021, doi: 10.1007/s41133-020-00043-x.

[27] J. Sohn, G.-W. Kim, and S.-B. Choi, "A state-of-the-art review on robots and medical devices using smart fluids and shape memory alloys," *Appl. Sci.*, vol. 8, no. 10, p. 1928, Oct. 2018, doi: 10.3390/app8101928.

[28] M. S. Rahmat, K. Hudha, Z. A. Kadir, N. H. Amer, N. R. M. Nuri, and S. Abdullah, "Modelling and characterization of a magneto-rheological elastomer isolator device under impact loadings using interpolated multiple adaptive neuro fuzzy inference system structure," *Int. J. Mater. Struct. Integrity*, vol. 13, no. 4, pp. 215–241, 2019, doi: 10.1504/IJMSI.2019.103210.

[29] S. Ravishankar and R. Mahale, "A study on magneto rheological fluids and their applications," *Int. Res. J. Eng. Technol.*, vol. 2, no. 4, pp. 2023–2028, 2015.

[30] A. N. Kulkarni and S. R. Patil, "Magneto-rheological (MR) and electro-rheological (ER) fluid damper: A review parametric study of fluid behavior," *Int. J. Eng. Res. Appl.*, vol. 3, no. 6, pp. 1879–1882, 2013.

[31] K. S. Arsava and Y. Kim, "Modeling of magnetorheological dampers under various impact loads," *Shock Vibrat.*, vol. 2015, pp. 1–20, Jan. 2015, doi: 10.1155/2015/905186.

[32] K. Özsoy and M. R. Usal, "A mathematical model for the magnetorheological materials and magneto reheological devices," *Eng. Sci. Technol., Int. J.*, vol. 21, no. 6, pp. 1143–1151, Dec. 2018, doi: 10.1016/j.jestch.2018.07.019.

[33] J. Park, G. H. Yoon, J. W. Kang, and S. B. Choi, "Design and control of a prosthetic leg for above-knee amputees operated in semi-active and active modes," *Smart Mater. Struct.*, vol. 25, no. 8, 2016, Art. no. 085009, doi: 10.1088/0964-1726/25/8/085009.

[34] A. R. Bhise, R. G. Desai, M. R. N. Yerrawar, A. C. Mitra, and D. R. R. Arakerimath, "Comparison between passive and semi-active suspension system using MATLAB/simulink," *IOSR J. Mech. Civil Eng.*, vol. 13, no. 4, pp. 1–6, Apr. 2016, doi: 10.9790/1684-1304010106.

[35] B. G. Kavyashree, S. Patil, and V. S. Rao, "Evolution of outrigger structural system: A state-of-the-art review," *Arabian J. Sci. Eng.*, vol. 46, no. 11, pp. 10313–10331, Nov. 2021, doi: 10.1007/s13369-021-06074-9.

[36] D. Hua, X. Liu, Z. Li, P. Fracz, A. Hnydiuk-Stefan, and Z. Li, "A review on structural configurations of magnetorheological fluid based devices reported in 2018–2020," *Frontiers Mater.*, vol. 8, pp. 1–15, Mar. 2021, doi: 10.3389/fmats.2021.640102.

[37] M. Rahman, Z. C. Ong, S. Julai, M. M. Ferdaus, and R. Ahamed, "A review of advances in magnetorheological dampers: Their design optimization and applications," *J. Zhejiang Univ.-Sci. A*, vol. 18, no. 12, pp. 991–1010, Dec. 2017, doi: 10.1631/jzus.A1600721.

[38] J.-S. Oh and S.-B. Choi, "State of the art of medical devices featuring smart electro-rheological and magneto-rheological fluids," *J. King Saud Univ.-Sci.*, vol. 29, no. 4, pp. 390–400, Oct. 2017, doi: 10.1016/j.jksus.2017.05.012.

[39] S. A. Khan, A. Suresh, and N. SeethaRamaiah, "Principles, characteristics and applications of magneto rheological fluid damper in flow and shear mode," *Proc. Mater. Sci.*, vol. 6, pp. 1547–1556, Jan. 2014, doi: 10.1016/j.mspro.2014.07.136.

[40] S. L. Ntella, K. Jeanmonod, M.-T. Duong, Y. Civet, C. Koechli, and Y. Perriard, "Preliminary study of pressure self-sensing miniature magnetorheological valves," in *Proc. IEEE/ASME Int. Conf. Adv. Intell. Mechatronics (AIM)*, Jul. 2021, pp. 606–611, doi: 10.1109/AIM46487.2021.9517656.

[41] A. Naseri, M. M. Moghaddam, M. Gharini, and M. A. Sharbafi, "A novel adjustable damper design for a hybrid passive ankle prosthesis," *Actuat.*, vol. 9, no. 3, p. 74, 2020, doi: 10.3390/act9030074.

[42] M. Kubík, O. Macháček, Z. Strecker, J. Roupec, and I. Mazurek, "Design and testing of magnetorheological valve with fast force response time and great dynamic force range," *Smart Mater. Struct.*, vol. 26, no. 4, Apr. 2017, Art. no. 047002, doi: 10.1088/1361-665X/aa6066.

[43] C. Han, S.-B. Choi, Y.-S. Lee, H.-T. Kim, and C.-H. Kim, "A new hybrid Mount actuator consisting of air spring and magneto-rheological damper for vibration control of a heavy precision stage," *Sens. Actuators A, Phys.*, vol. 284, pp. 42–51, Dec. 2018, doi: 10.1016/j.sna.2018.10.020.

[44] H. Lv, S. Zhang, Q. Sun, R. Chen, and W. J. Zhang, "The dynamic models, control strategies and applications for magnetorheological damping systems: A systematic review," *J. Vibrat. Eng. Technol.*, vol. 9, no. 1, pp. 131–147, Jan. 2021, doi: 10.1007/s42417-020-00215-4.

[45] Q. Fu, D.-H. Wang, L. Xu, and G. Yuan, "A magnetorheological damper-based prosthetic knee (MRPK) and sliding mode tracking control method for an MRPK-based lower limb prosthesis," *Smart Mater. Struct.*, vol. 26, no. 4, Apr. 2017, Art. no. 045030, doi: 10.1088/1361-665X/aa61f1.

[46] Z. Safaeepour, A. Eshraghi, and M. Geil, "The effect of damping in prosthetic ankle and knee joints on the biomechanical outcomes: A literature review," *Prosthetics Orthotics Int.*, vol. 41, no. 4, pp. 336–344, 2017, doi: 10.1177/0309364616677651.

[47] R. M. de Andrade, J. S. R. Martins, M. Pinotti, A. B. Filho, and C. B. S. Vimieiro, "Novel active magnetorheological knee prosthesis presents low energy consumption during ground walking," *J. Intell. Mater. Syst. Struct.*, vol. 32, no. 14, pp. 1591–1603, Aug. 2021, doi: 10.1177/1045389X20983923.

[48] L. D. A. Paulo, A. B. Filho, C. Vimieiro, and R. M. Andrade, "Transient thermal analysis of a MR clutch for knee prostheses and exoskeletons," Tech. Rep., Feb. 2018, doi: 10.26678/ABCM.COBEM2017.COB17-0311.

[49] H. Yu, W. Cao, Q. Meng, W. Chen, and S. Li, "Physiological parameters analysis of transfemoral amputees with different prosthetic knees," *Acta Bioeng. Biomech.*, vol. 21, no. 3, pp. 135–142, 2019, doi: 10.5277/ABB-01321-2019-02.

[50] J. H. Campbell, P. M. Stevens, and S. R. Wurdeman, "OASIS 1: Retrospective analysis of four different microprocessor knee types," *J. Rehabil. Assistive Technol. Eng.*, vol. 7, Jan. 2020, Art. no. 205566832096847, doi: 10.1177/2055668320968476.

[51] T. Oba, H. Kadone, M. Hassan, and K. Suzuki, "Robotic ankle-foot orthosis with a variable viscosity link using MR fluid," *IEEE/ASME Trans. Mechatronics*, vol. 24, no. 2, pp. 495–504, Apr. 2019, doi: 10.1109/TMECH.2019.2894406.

[52] Y. C. A. Hutabarat, K. Ekkachai, and W. Kongprawechnon, "Knee torque estimation in non-pathological gait using dynamics modelling and feed-forward neural network," in *Proc. 56th Annu. Conf. Soc. Instrum. Control Engineers Jpn. (SICE)*, Sep. 2017, pp. 1297–1302, doi: 10.23919/SICE.2017.8105605.

[53] Y. Zhang, J. Wang, W. Li, J. Wang, and P. Yang, "A model-free control method for estimating the joint angles of the knee exoskeleton," *Adv. Mech. Eng.*, vol. 10, no. 10, pp. 1–10, 2018, doi: 10.1177/1687814018807768.

[54] R. Leskovar, A. Körner, and F. Breitenecker, "Simulation case study: Using simscape for human knee joint models," *SNE Simul. Notes Eur.*, vol. 29, no. 2, pp. 101–104, Jun. 2019, doi: 10.11128/sne.29.sn.10477.

[55] A. Rossi, F. Orsini, A. Scorza, F. Botta, N. Belfiore, and S. Sciuto, "A review on parametric dynamic models of magnetorheological dampers and their characterization methods," *Actuators*, vol. 7, no. 2, p. 16, Apr. 2018, doi: 10.3390/act7020016.

[56] R. Ahamed, M. M. Ferdaus, and Y. Li, "Advancement in energy harvesting magneto-rheological fluid damper: A review," *Korea-Aust. Rheol. J.*, vol. 28, no. 4, pp. 355–379, Nov. 2016, doi: 10.1007/s13367-016-0035-2.

[57] R. M. Desai, M. E. H. Jamadar, H. Kumar, S. Joladarashi, S. C. Rajasekaran, and G. Amarnath, "Evaluation of a commercial MR damper for application in semi-active suspension," *Social Netw. Appl. Sci.*, vol. 1, no. 9, pp. 1–10, Sep. 2019, doi: 10.1007/s42452-019-1026-y.

[58] H. Sayyaadi and S. H. Zareh, "Intelligent control of an MR prosthesis knee using of a hybrid self-organizing fuzzy controller and multidimensional wavelet NN," *J. Mech. Sci. Technol.*, vol. 31, no. 7, pp. 3509–3518, Jul. 2017, doi: 10.1007/s12206-016-1236-9.

[59] R. S. T. Saini, H. Kumar, and S. Chandramohan, "Semi-active control of a swing phase dynamic model of transfemoral prosthetic device based on inverse dynamic model," *J. Brazilian Soc. Mech. Sci. Eng.*, vol. 42, no. 6, pp. 1–14, Jun. 2020, doi: 10.1007/s40430-020-02387-2.

[60] S. Seid, S. Chandramohan, and S. Sujatha, "Optimal design of an MR damper valve for prosthetic knee application," *J. Mech. Sci. Technol.*, vol. 32, no. 6, pp. 2959–2965, Jun. 2018, doi: 10.1007/s12206-018-0552-7.

[61] Y. B. Kazakov, N. A. Morozov, and S. A. Nesterov, "Development of models of the magnetorheological fluid damper," *J. Magn. Magn. Mater.*, vol. 431, pp. 269–272, Jun. 2017, doi: 10.1016/j.jmmm.2016.10.006.

[62] Y. Shiao and P. Gadde, "Investigation of hysteresis effect in torque performance for a magnetorheological brake in adaptive knee orthosis," *Actuators*, vol. 10, no. 10, p. 271, Oct. 2021, doi: 10.3390/act10100271.

[63] S. K. Lohit, K. Hemanth, H. Kumar, and K. V. Gangadharan, "Experimental and analytical studies on magnetorheological damper," *Appl. Mech. Mater.*, vol. 854, pp. 127–132, Oct. 2016, doi: 10.4028/www.scientific.net/amm.854.127.

[64] W. Elsaady, S. O. Oyadiji, and A. Nasser, "A one-way coupled numerical magnetic field and CFD simulation of viscoplastic compressible fluids in MR dampers," *Int. J. Mech. Sci.*, vol. 167, Feb. 2020, Art. no. 105265, doi: 10.1016/j.ijmecsci.2019.105265.

[65] A. Tognetti, F. Lorussi, N. Carbonaro, and D. de Rossi, "Wearable goniometer and accelerometer sensory fusion for knee joint angle measurement in daily life," *Sensors*, vol. 15, no. 11, pp. 28435–28455, Nov. 2015, doi: 10.3390/s151128435.

[66] C. N. Teague, S. Hersek, H. Töreyin, M. L. Millard-Stafford, M. L. Jones, G. F. Kogler, M. N. Sawka, and O. T. Inan, "Novel methods for sensing acoustical emissions from the knee for wearable joint health assessment," *IEEE Trans. Biomed. Eng.*, vol. 63, no. 8, pp. 1581–1590, Aug. 2016, doi: 10.1109/TBME.2016.2543226.

[67] B. Sawaryn, N. Piaseczna, S. Sieciński, R. Doniec, K. Duraj, D. Komorowski, and E. J. Tkacz, "The assessment of the condition of knee joint surfaces with acoustic emission analysis," *Sensors*, vol. 21, no. 19, p. 6495, Sep. 2021, doi: 10.3390/S21196495.

[68] C. T.-S. Ching, S.-Y. Liao, T.-Y. Cheng, C.-H. Cheng, T.-P. Sun, Y.-D. Yao, C.-S. Hsiao, and K.-M. Chang, "A mechanical sensor designed for dynamic joint angle measurement," *J. Healthcare Eng.*, vol. 2017, pp. 1–12, Jan. 2017, doi: 10.1155/2017/8465212.

[69] T. Lockhart, *Sensors for Gait, Posture, and Health Monitoring*, vol. 1. 2020, doi: 10.3390/books978-3-03936-347-6.

[70] P. Van Thanh, D.-T. Tran, D.-C. Nguyen, N. D. Anh, D. N. Dinh, S. El-Rabaie, and K. Sandrasegaran, "Development of a real-time, simple and high-accuracy fall detection system for elderly using 3-DOF accelerometers," *Arabian J. Sci. Eng.*, vol. 44, no. 4, pp. 3329–3342, Aug. 2018, doi: 10.1007/S13369-018-3496-4.

[71] J.-Y. Jung, W. Heo, H. Yang, and H. Park, "A neural network-based gait phase classification method using sensors equipped on lower limb exoskeleton robots," *Sensors*, vol. 15, no. 11, pp. 27738–27759, Oct. 2015, doi: 10.3390/s151127738.

[72] R. Radakovic and N. Filipovic, "Sport biomechanics: Experimental and computer simulation of knee joint during jumping and walking," in *Computational Modeling in Bioengineering and Bioinformatics*. Amsterdam, The Netherlands: Elsevier, 2020, pp. 387–418, doi: 10.1016/b978-0-12-819583-3.00012-6.

[73] E. Papi, Y. N. Bo, and A. H. McGregor, "A flexible wearable sensor for knee flexion assessment during gait," *Gait Posture*, vol. 62, pp. 480–483, May 2018, doi: 10.1016/j.gaitpost.2018.04.015.

[74] Z. A. Abro, Z. Yi-Fan, C. Nan-Liang, H. Cheng-Yu, R. A. Lakho, and H. Halepoto, "A novel flex sensor-based flexible smart garment for monitoring body postures," *J. Ind. Textiles*, vol. 49, no. 2, pp. 262–274, Aug. 2019, doi: 10.1177/1528083719832854.

[75] Y. Feng, Y. Li, D. McCoul, S. Qin, T. Jin, B. Huang, and J. Zhao, "Dynamic measurement of legs motion in sagittal plane based on soft wearable sensors," *J. Sensors*, vol. 2020, pp. 1–10, Feb. 2020, doi: 10.1155/2020/9231571.

[76] V. Chhoeum, Y. Kim, and S.-D. Min, "Estimation of knee joint angle using textile capacitive sensor and artificial neural network implementing with three shoe types at two gait speeds: A preliminary investigation," *Sensors*, vol. 21, no. 16, p. 5484, Aug. 2021, doi: 10.3390/s21165484.

[77] S. Pandit, A. Godiyal, A. Vimal, U. Singh, D. Joshi, and D. Kalyanasundaram, "An affordable insole-sensor-based trans-femoral prosthesis for normal gait," *Sensors*, vol. 18, no. 3, p. 706, 2018, doi: 10.3390/S18030706.

[78] M. Versteyhe, H. De Vroey, F. Debrouwere, H. Hallez, and K. Claeys, "A novel method to estimate the full knee joint kinematics using low cost IMU sensors for easy to implement low cost diagnostics," *Sensors*, vol. 20, no. 6, p. 1683, Mar. 2020, doi: 10.3390/s20061683.

[79] B. H. Kim, S. H. Hong, I. W. Oh, Y. W. Lee, I. H. Kee, and S. Y. Lee, "Measurement of ankle joint movements using IMUs during running," *Sensors*, vol. 21, no. 12, p. 4240, Jun. 2021, doi: 10.3390/S21124240.

[80] X. Wang, H. Yu, S. Kold, O. Rahbek, and S. Bai, "Wearable sensors for activity monitoring and motion control: A review," *Biomimetic Intell. Robot.*, vol. 3, no. 1, Mar. 2023, Art. no. 100089, doi: 10.1016/J.BIROB.2023.100089.

[81] C. R. Hollis, R. M. Koldenhoven, J. E. Resch, and J. Hertel, "Running biomechanics as measured by wearable sensors: Effects of speed and surface," *Sports Biomechanics*, vol. 20, no. 5, pp. 521–531, Jul. 2021, doi: 10.1080/14763141.2019.1579366.

[82] C. X. Tong and M. S. H. Bhuiyan, "An investigation into a locking mechanism designed for a gear-based knee joint prosthesis," *Cogent Eng.*, vol. 7, no. 1, Jan. 2020, Art. no. 1738186, doi: 10.1080/23311916.2020.1738186.

[83] M. R. Tucker, J. Olivier, A. Pagel, H. Bleuler, M. Bouri, O. Lambercy, J. D. R. Millán, R. Riener, H. Vallery, and R. Gassert, "Control strategies for active lower extremity prosthetics and orthotics: A review," *J. NeuroEng. Rehabil.*, vol. 12, no. 1, pp. 1–30, 2015, doi: 10.1186/1743-0003-12-1.

[84] Z. Choffin, N. Jeong, M. Callihan, S. Olmstead, E. Sazonov, S. Thakral, C. Getchell, and V. Lombardi, "Ankle angle prediction using a footwear pressure sensor and a machine learning technique," *Sensors*, vol. 21, no. 11, p. 3790, May 2021, doi: 10.3390/S21113790.

[85] C. Ochoa-Diaz, T. S. Rocha, L. D. L. Oliveira, M. G. Paredes, R. Lima, A. P. L. Bó, and G. A. Borges, "An above-knee prosthesis with magnetorheological variable-damping," in *Proc. 5th IEEE RAS/EMBS Int. Conf. Biomed. Robot. Biomechatronics*, 2014, pp. 108–113, doi: 10.1109/biorob.2014.6913761.

[86] D. Adiputra, M. A. A. Rahman, I. Bahiuddin, F. Imaduddin, and N. Nazmi, "Sensor number optimization using neural network for ankle foot orthosis equipped with magnetorheological brake," *Open Eng.*, vol. 11, no. 1, pp. 91–101, Nov. 2020, doi: 10.1515/eng-2021-0010.

[87] M. Sharbafi, A. Naseri, A. Seyfarth, and M. Grimmer, "Neural control in prostheses and exoskeletons," in *Powered Prostheses*. Amsterdam, The Netherlands: Elsevier, 2020, doi: 10.1016/B978-0-12-817450-0.00007-9.

[88] N. Nazmi, M. A. A. Rahman, S. A. Mazlan, D. Adiputra, I. Bahiuddin, M. K. Shabdin, N. A. A. Razak, and M. H. M. Ariff, "Analysis of EMG signals during stance and swing phases for controlling magnetorheological brake applications," *Open Eng.*, vol. 11, no. 1, pp. 112–119, Nov. 2020, doi: 10.1515/eng-2021-0009.

[89] N. Y. Sattar, Z. Kausar, S. A. Usama, U. Farooq, and U. S. Khan, "EMG based control of transhumeral prosthesis using machine learning algorithms," *Int. J. Control, Autom. Syst.*, vol. 19, no. 10, pp. 3522–3532, Oct. 2021, doi: 10.1007/s12555-019-1058-5.

[90] R. Gupta and R. Agarwal, "Electromyographic signal-driven continuous locomotion mode identification module design for lower limb prosthesis control," *Arabian J. Sci. Eng.*, vol. 43, no. 12, pp. 7817–7835, Mar. 2018, doi: 10.1007/S13369-018-3193-3.

[91] Q. Zuo, J. Zhao, X. Mei, F. Yi, and G. Hu, "Design and trajectory tracking control of a magnetorheological prosthetic knee joint," *Appl. Sci.*, vol. 11, no. 18, p. 8305, Sep. 2021, doi: 10.3390/app11188305.

[92] W. Cao, H. Yu, W. Chen, Q. Meng, and C. Chen, "Design and evaluation of a novel microprocessor-controlled prosthetic knee," *IEEE Access*, vol. 7, pp. 178553–178562, 2019, doi: 10.1109/ACCESS.2019.2957823.

[93] A. Bavarsad, A. Fakharian, and M. B. Menhaj, "Optimal sliding mode controller for an active transfemoral prosthesis using state-dependent Riccati equation approach," *Arabian J. Sci. Eng.*, vol. 45, no. 8, pp. 6559–6572, Aug. 2020, doi: 10.1007/s13369-020-04563-x.

[94] Y. Feng, W. Chen, and Q. Wang, "A strain gauge based locomotion mode recognition method using convolutional neural network," *Adv. Robot.*, vol. 33, no. 5, pp. 254–263, Mar. 2019, doi: 10.1080/01691864.2018.1563500.

[95] Y. Hutabarat, K. Ekkachai, M. Hayashibe, and W. Kongprawechnon, "Reinforcement Q-learning control with reward shaping function for swing phase control in a semi-active prosthetic knee," *Frontiers Neurorobotics*, vol. 14, pp. 1–10, Nov. 2020, doi: 10.3389/fnbot.2020.565702.

[96] J. D. Farah, N. Baddour, and E. D. Lemaire, "Design, development, and evaluation of a local sensor-based gait phase recognition system using a logistic model decision tree for orthosis-control," *J. NeuroEng. Rehabil.*, vol. 16, no. 1, pp. 1–11, Dec. 2019, doi: 10.1186/s12984-019-0486-z.

[97] H. Xie, G. Li, and F. Li, "Modeling of magnetorheological damper and fuzzy PID control of intelligent bionic leg with meniscus," in *Proc. WRC Symp. Adv. Robot. Autom. (WRC SARA)*, Aug. 2019, pp. 387–393, doi: 10.1109/WRC-SARA.2019.8931965.

[98] N. D. Nordin, A. G. Muthalif, and M. K. M. Razali, "Control of transtibial prosthetic limb with magnetorheological fluid damper by using a fuzzy PID controller," *J. Low Freq. Noise, Vibrat. Act. Control*, vol. 37, no. 4, pp. 1067–1078, Dec. 2018, doi: 10.1177/1461348418766171.

[99] D. Adiputra, N. Nazmi, I. Bahiuddin, U. Ubaidillah, F. Imaduddin, M. A. A. Rahman, S. A. Mazlan, and H. Zamzuri, "A review on the control of the mechanical properties of ankle foot orthosis for gait assistance," *Actuators*, vol. 8, no. 1, p. 10, 2019, doi: 10.3390/act8010010.

[100] G. Liu, F. Gao, D. Wang, and W.-H. Liao, "Medical applications of magnetorheological fluid: A systematic review," *Smart Mater. Struct.*, vol. 31, no. 4, Apr. 2022, Art. no. 043002, doi: 10.1088/1361-665X/ac54e7.

AKHILA BHAT received the Bachelor of Engineering and master's degrees in instrumentation and control engineering and control system from the Manipal Institute of Technology, India, in 2017 and 2019, respectively. She is currently pursuing the Ph.D. degree in biomechanics and control. She has three conference paper publications in her credit. Her research interests include observer design and intelligent estimation.

VIDYA S. RAO (Member, IEEE) received the Bachelor of Engineering degree in electrical and electronics from the Karnataka Regional Engineering College, Surathkal, in 1996, the master's degree in control systems from the Manipal Institute of Technology, Manipal Academy of Higher Education (MAHE), Manipal, and the Ph.D. degree from MAHE, in 2017. She is currently an Associate Professor with the Department of Instrumentation and Control Engineering, Manipal Institute of Technology, MAHE. She is a member of the Indian Society for Science and Engineering (ISSE). She has published more than 22 technical papers in reputed international journals and conferences. Her research interests include observer-based controller design and semiactive control using MR dampers for outrigger structures.

N. S. JAYALAKSHMI (Senior Member, IEEE) received the B.E. degree in electrical engineering from MSRIT, Bengaluru, India, in 1991, the M.Tech. degree in power systems from the National Institute of Engineering, Mysore, India, in 1999, and the Ph.D. degree from the Department of Electrical and Electronics Engineering, National Institute of Technology, Karnataka, Surathkal, India. She is currently a Professor with the Department of Electrical and Electronics Engineering, Manipal Institute of Technology, Manipal Academy of Higher Education, India. She has published more than 75 technical papers in reputed international journals and conferences. She is a Senior Member of PES and a Life Member of ISTE and SSI. Her research interests include power system operation and control, distributed generation systems, the control of microgrids, and electric vehicles.